



Spatiotemporal Variability in Sedimentation Drives Habitat Loss on Restored Subtidal Oyster Reefs

Olivia N. Caretti^{1,2} · DelWayne R. Bohnenstiehl^{1,3} · David B. Eggleston^{1,2}

Received: 29 May 2020 / Revised: 17 February 2021 / Accepted: 23 February 2021 / Published online: 17 March 2021
© Coastal and Estuarine Research Federation 2021

Abstract

Restored oyster reefs enhance commercial harvests and ecosystem services in coastal environments. Spatial and temporal changes in habitat availability can affect reef persistence and restoration benefits, and understanding how construction and location of a restored habitat influence its persistence over time is key to optimizing restoration efforts. The short-term persistence of six subtidal restored oyster reefs in Pamlico Sound, NC, USA was characterized by sidescan sonar and bathymetric mapping conducted immediately after restoration in August 2016 and again 21 months later in May 2018. A U-net convolutional neural network architecture was trained to classify reef pixels within the sonar imagery using image-based and image-texture features calculated from gray-level co-occurrence matrices. Oyster reef restoration used shell and limestone marl to construct flat substrates, with only a few 10's of centimeters of local relief, spread over areas of ~3000–12,000 m². All six reefs provided habitat for the settlement and growth of oyster populations, but this role changed as reefs underwent varying degrees of sediment burial between surveys. Reefs constructed in relatively low-energy environments lost ~18–35% of their substrate area, primarily by deposition of sediment along their margins. Reefs having greater sediment supply and greater exposure to predominant winds and currents were most susceptible to burial and became heavily fragmented with ~50–65% of the restored habitat lost. Sediment dynamics appear to exert a controlling influence on the success of these reefs, and oyster restoration sites in high-energy environments may have limited long-term economic and ecosystem benefits.

Keywords Oyster reef · Habitat restoration · Sedimentation · Sidescan sonar · Deep learning · Semantic segmentation

Introduction

Given that oysters and oyster reefs provide valuable ecosystem services and economic benefits, restoration of these degraded biogenic habitats has been a priority for several decades (Coen et al. 2007; Powers et al. 2009; Beck et al. 2011; Grabowski et al. 2012; La Peyre et al. 2014; Baggett et al. 2015; Hernández et al. 2018; Theuerkauf et al. 2019). Restoration seeks to enhance oyster populations (and indirectly, associated ecosystem

services) by increasing available substrate to supplement natural habitat for settling oysters, or deploying live oysters to areas with high growth and survivorship, yet low natural larval settlement (Beck et al. 2011; La Peyre et al. 2014; Baggett et al. 2015; Hernández et al. 2018). In many states along the US East and Gulf Coasts, both approaches are used to promote ecosystem services of oysters, support an oyster fishery, and promote economic growth (e.g., MD DNR 2020; NC DMF 2020a; VA DEQ 2020). Despite these efforts, only a marginal fraction of historic reefs have been successfully restored (Beck et al. 2011; Hernández et al. 2018).

In North Carolina, oyster reef restoration is a key priority outlined in the State's long-term Coastal Habitat Protection Plan (Deaton et al. 2010). The North Carolina Division of Marine Fisheries (NC DMF) has established two primary restoration programs to address this need. The Oyster Sanctuary Program has established a network of 15 no-harvest reserves that were constructed to provide larval spillover to harvested reefs. Reefs within the reserves are high relief (1–2 m) and are constructed with a variety of materials including recycled oyster and clam shell, limestone boulders, concrete reef balls, and

Communicated by Judy Grassle

✉ Olivia N. Caretti
oncarett@ncsu.edu

¹ Department of Marine, Earth, & Atmospheric Sciences, North Carolina State University, Raleigh, NC, USA

² Center for Marine Sciences and Technology, North Carolina State University, Morehead City, NC, USA

³ Center for Geospatial Analytics, North Carolina State University, Raleigh, NC, USA

granite rip rap (NC DMF 2020a). Most of these reserves support robust oyster populations, with some serving as metapopulation sinks and others as sources based on differences in larval production, connectivity, recruitment, and oyster survival (Powers et al. 2009; Mroch et al. 2012; Puckett and Eggleston 2012; Puckett et al. 2014; Puckett and Eggleston 2016; Peters et al. 2017).

In addition to these no-harvest reserves, the NC DMF annually builds dozens of lower relief (<0.5 m) habitats using limestone marl and recycled shell, collectively called cultch. These cultch reefs are constructed on sedimented substrates within shallow (<2–3 m) embayments and are intended to support oyster settlement and growth for harvest (Peters et al. 2017; NC DMF 2020a). They are open to commercial fishing (mechanical dredging and hand tonging) once oysters reach legal size (76-mm shell height), typically after ~3 years. The NC DMF annually deposits 3500–17,500 m³ of cultch in harvestable subtidal waters, with an estimated total of 700,000 m³ of material deployed between 1915, when oyster habitat enhancement efforts began in the state, and 2013 (Callihan et al. 2016).

The NC DMF identifies appropriate areas for restoration based on accessibility to reef material stockpiles and restoration sites, ease of access for commercial fishermen, and historic fishery knowledge. Although habitat suitability index (HSI) models (Puckett et al. 2018; Theuerkauf et al. 2019) are being used to guide placement of no-take, subtidal oyster spawning sanctuaries in NC, there is no HSI model to guide placement of cultch reefs (J. Peters, NC DMF, pers. comm.). The present study was designed, in part, to help inform creation of such an HSI model for siting cultch reefs.

Improved oyster demographics and the associated ecosystem benefits of oyster restoration for water quality improvement and fish habitat enhancement, among others, are well-known and have been cited as factors justifying the construction of subtidal reefs in North Carolina (e.g., Powers et al. 2009; Pierson and Eggleston 2014; Peters et al. 2017; Theuerkauf et al. 2019). The North Carolina Cultch Planting Program is a substantial investment—costing ~\$10 million in 2010–2015—and the acreage and benefits provided by previously constructed cultch reefs are assumed to persist long-term once restoration is complete (Callihan et al. 2016). However, issues with sedimentation and hypoxia on low-relief subtidal reefs in North Carolina are common and can occur relatively quickly—even before harvest begins (Lenihan and Peterson 1998; Lenihan 1999; Powers et al. 2009; Peters et al. 2017). Since existing measures of restoration benefits do not account for these rapid changes in habitat quality, long-term expected benefits are likely overestimated. The longevity of cultch reefs should be quantified before benefits can be properly evaluated (Grabowski et al. 2012).

Here, we quantify the short-term persistence of restored low-relief oyster cultch reefs in a relatively shallow, wind-

driven lagoonal-type estuary. Newly constructed reefs were mapped twice over a period of ~21 months using a high-resolution (550 kHz/1600 kHz) bathymetric and side-scanning sonar system. Semantic segmentation of the sonar imagery was accomplished using a deep learning network operating on a suite of image and image-based textural feature classes. To assess reef longevity, and inform future reef design and construction efforts, temporal and spatial changes in reef substrate were explored as a function of location and site characteristics. We conclude with recommendations for incorporating sediment processes into oyster restoration siting.

Study System

Pamlico Sound (~120 km × 40 km) is a shallow (~4.5-m average depth) lagoonal estuary with limited tidal influence from its three narrow oceanic inlets. Our study was conducted on a set of six subtidal restored oyster cultch reefs (hereafter, reefs) that were constructed by the NC Division of Marine Fisheries (NC DMF) Cultch Planting Program in the summer of 2016 (Fig. 1; Table 1). These reefs are located within southwestern Pamlico Sound, near its confluence with the Pamlico and Neuse River estuaries.

The Pamlico River Estuary covers ~2600 km² and includes the Pungo River and lower Tar-Pamlico River (NC DWR 2014). The Neuse River Estuary covers ~1500 km² and includes the lower Neuse and Bay Rivers (NC DWR 2009). Both river-estuarine systems drain ~16,000 km² of the central-eastern piedmont and coastal plains, including substantial agricultural areas. They are often characterized by high turbidity, high nutrient loads, and low DO events, especially following increasingly frequent major storms (Paerl et al. 1998, 2018; Burkholder et al. 2004; NC DWR 2009, 2014).

During the present study, base-level discharge fluctuated around 50 m³ s⁻¹ and 75 m³ s⁻¹ for the Tar-Pamlico and Neuse Rivers, respectively (Fig. S1; USGS stations 02089500 and 02083500). Hurricane Matthew (category 1), however, caused historic flooding in October 2016, with mean daily discharges reaching ~1200 and ~1000 m³ s⁻¹ (Fig. S1). This marked the second highest period of discharge observed since monitoring began in the 1930s—being surpassed only during the passage of Hurricane Floyd in 1999 (Fig. S1; USGS stations 02089500 and 02083500). Riverine flushing associated with the passage of Hurricane Matthew delivered a pulse of high turbidity water into the estuary and altered the hydrodynamic and biogeochemical processes of southern Pamlico Sound for 2–3 months (Paerl et al. 2018, 2020; Du et al. 2019; Osburn et al. 2019). In late April 2017, following an atmospheric front which brought heavy rain, mean daily discharge from both rivers rose again to ~550 m³ s⁻¹; discharge events of this size or larger occur on average every ~4 years (Fig. S1).

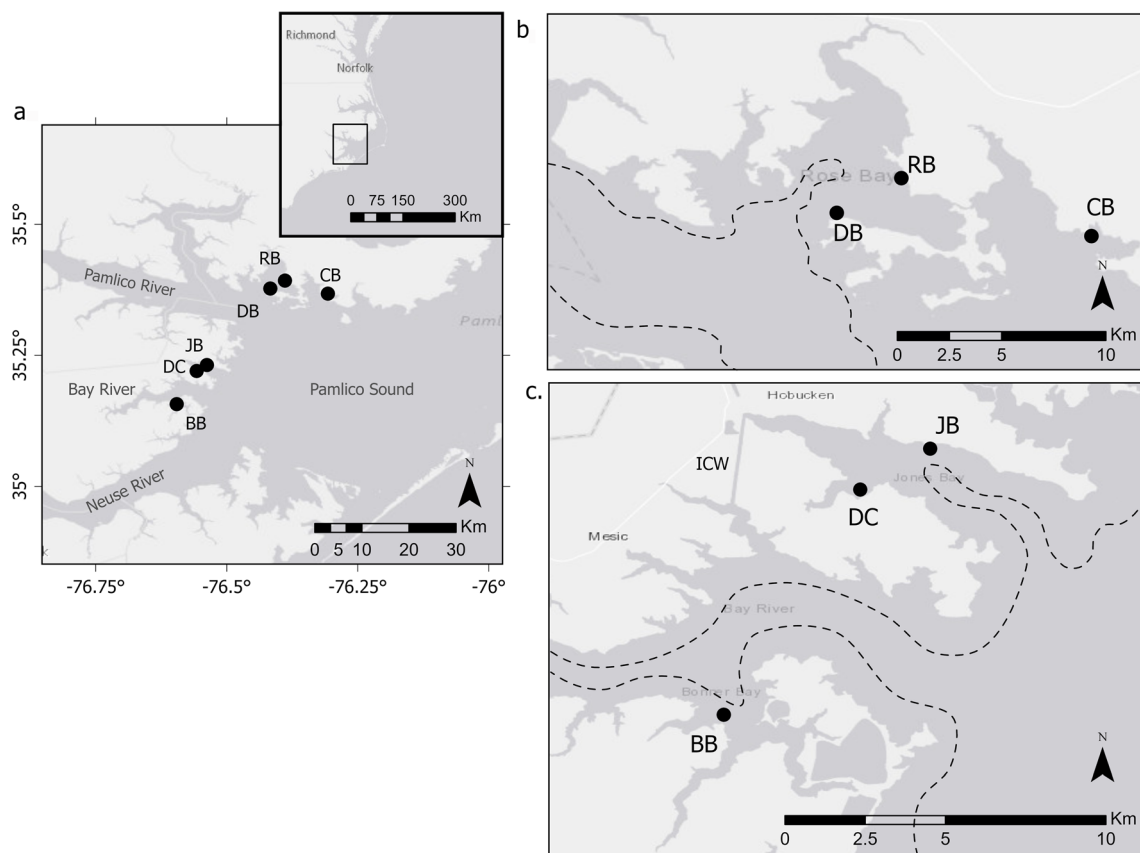


Fig. 1 **a** Study reefs in southwest Pamlico Sound, NC, USA. **b** Northern reefs: Deep Bay (DB), Rose Bay (RB), and Caffee Bay (CB). **c** Southern reefs: Bonner Bay (BB), Ditch Creek (DC), and Jones Bay (JB). Dashed

lines in **b** and **c** represent approximate deep channel isobaths (4–6 m depth) for both river-estuarine systems

Winds in coastal North Carolina are southwesterly (toward northeast) in the summer, and northeasterly (toward southwest) or northwesterly (toward southeast) in the fall, winter, and early spring (Xie and Eggleston 1999; Luettich et al. 2002; Jia and Li 2012b). Median wind speeds are $\sim 4.7 \text{ m s}^{-1}$, but often exceed $\sim 12 \text{ m s}^{-1}$ (95% quantile) during the

passage of atmospheric fronts, hurricanes, and nor'easters (Fig. S2). Wind strength and direction drive sediment resuspension within Pamlico Sound (Paerl et al. 2006; Mulligan et al. 2015; Clunies et al. 2017) and the local exposure of shorelines to wind and wave energy is a primary factor controlling their erosion (Coward et al. 2011; Eulie et al. 2017).

Table 1 Reef location and construction information. Initial volume (m^3) of material for sites with mixed substrates listed as marl (M), shell (S), and total volume (T)

Site name	Site ID	Location	Material	Initial volume (m^3)
Bonner Bay	BB	South	Mixed	M: 687 S: 274 T: 961
Ditch Creek	DC	South	Mixed	M: 357 S: 39 T: 397
Jones Bay	JB	South	Marl	262
Deep Bay	DB	North	Marl	469
Rose Bay	RB	North	Shell	579
Caffee Bay	CB	North	Shell	637

Water circulation near the study sites is driven primarily by wind (Xie and Eggleston 1999; Luettich et al. 2002; Jia and Li 2012a, b) and freshwater input from the Tar-Pamlico and Neuse river systems. Modeling suggests that during southwesterly and northwesterly winds, surface waters in southwestern Pamlico Sound generally flow eastward away from the rivers as bottom waters move westward toward the rivers (Xie and Eggleston 1999; Jia and Li 2012b). During northeasterly winds, water flow becomes more complicated in the sub-bays and riverine estuaries, but generally moves southward at the surface and northward or eastward at depth (Jia and Li 2012b). Silts and clays sourced by riverine input and shoreline erosion are resuspended during strong wind events and transported locally over short distances by these currents (Wells and Kim 1989; Leonard et al. 1995; Giffin and Corbett 2003; Ji and Jin 2014). Although the specific pathways of sediment transport are not well-understood, these sediments are thought to be deposited and resuspended multiple

times en route to the deep basin. Sands are transported into Pamlico Sound through inlets and accumulate as flood tide deltas (Wells and Kim 1989).

Reef Construction

Reefs at Bonner Bay, Jones Bay, and Ditch Creek (southern reefs) were built south of the Pamlico River near the mouth of the Neuse River Estuary (Table 1; Fig. 1c). Bonner Bay is located within a sub-bay on the south side of the Bay River system. Three substantial marsh creeks flow into Bonner Bay before entering the Bay River proper. Reefs at Jones Bay and Ditch Creek were built in Jones Bay, which empties directly into Pamlico Sound. The Jones Bay reef is on the northern side of Jones Bay, and Ditch Creek is on the southern shore at the mouth of a marsh creek. The Intracoastal Waterway shipping channel intersects the head of Jones Bay and enters the lower-central part of the Bay River from the north. Reefs at Deep Bay, Caffee Bay, and Rose Bay (northern reefs) were built in sub-bays north of the confluence of the Pamlico River with Pamlico Sound (Fig. 1b). Given the different hydrodynamic features and sources of water to these areas, southern and northern reefs were expected to have different abiotic regimes and develop differently.

Seabed sediments throughout western Pamlico Sound typically comprise a mixture of sand, silt, and clay size particles (Poppe et al. 2014; Eulie et al. 2018). The NC DMF has mapped benthic habitat throughout portions of western Pamlico Sound using a sounding pole to characterize the substrate sediments as soft, firm, or hard based on the refusal of the pole (NC DMF 2020b). Soundings were conducted from a small GPS-equipped vessel traversing initially along gridlines at 10-s intervals in latitude and longitude, and then employing finer resolution transects in areas where changes in the bottom characteristics were detected. The reefs mapped in this study were sited on hard substrate, with the Bonner Bay and Ditch Creek reefs positioned nearest to a transition between soft and hard sediments (Fig. S3).

Reefs were constructed in ~1–3 m of water with their margins ~100–200 m from the nearest saltmarsh. Reefs were built from recycled oyster shell, limestone marl, or a mix of both materials. Mixed reefs were constructed with a marl base and relatively thin shell veneer. Reefs were built by unevenly spraying material from a barge or by dumping material overboard using a bucket-loader. The total amount of material deployed to construct reefs varied between ~250 and 1000 m³ (Table 1).

Methods

Data Collection and Processing

To identify how reefs changed following restoration, they were mapped within a few weeks of construction in August 2016,

and then again 21 months later, in May 2018. Both surveys were conducted using a *SeaRobotics Mini-Cat* unmanned surface vehicle (USV) equipped with an *Edgetech* 6205 bathymetric side-scanning sonar (550 kHz/1600 kHz) that was mounted between the catamaran hulls. The USV was operated autonomously along pre-planned survey routes with the aid of a Hemisphere Vector 320 GPS (<20-cm horizontal accuracy). The shallow draft (<0.2 m) of the USV and the wide (>8× water depth) effective swath width of the sonar provided >100% bathymetric coverage and nearly 200% sidescan coverage over the planned footprint of the reef. Vehicle track lines were modified slightly between surveys to optimize the performance of the USV under prevailing sea states and to ensure full coverage of the reef area. Motion reference and position data were integrated with the sonar data in real time. Bathymetric returns were stored at 0.15-m range intervals, and dual-frequency sonar data (550 kHz/1600 kHz) were acquired using the HYPACK (v. 2016 and 2018) acquisition system. Sound velocity data were obtained from conductivity, temperature, and depth (CTD) profiles collected during the USV surveys.

Bathymetric data were post-processed using the MBMAX module with HYPACK (v. 2018), where navigation, motion reference, and point cloud data were manually reviewed and edited. Beam positions were recalculated based on local sound velocity data derived from the CTD profiles. Geo-referenced point cloud data were gridded with 0.5 × 0.5-m resolution using the MB-System package (Caress and Chayes 1995). Bottom-detection and navigation data were edited and smoothed before removing the water column from the sonar imagery. The intensity of the 1600-kHz sonar data was corrected with time-varying gain and swath data overlain to produce a sidescan mosaic with 0.05 × 0.05-m spatial resolution.

Classification of Reef Seabed

Sidescan Image Metrics

Due to differences in the acoustic impedance and fine-scale seabed roughness, reefs (recycled oyster shell, limestone marl, or a mix of both materials) were characterized by generally higher amplitude sonar returns compared with the surrounding sedimented seabed. However, even with such strong material contrasts, pixel-by-pixel thresholding based on intensity values is often an ineffective metric for image segmentation. This reflects (1) the use of normalized (rather than calibrated absolute) intensities when mosaics are created, (2) the heterogeneity of backscattered amplitudes and shadowing effects associated with seabed roughness and relief, and (3) the presence of various image artifacts related to the motion and geometry of the sonar.

To address some of these complicating factors, gray-level co-occurrence matrix (GLCM) methods introduced by

Haralick et al. (1973) have been used to segment sonar images (e.g., Pace and Dyer 1979; Reed and Hussong 1989; Blondel et al. 1998). In this approach, the texture of an image is characterized by calculating how often pairs of pixels with specific gray levels and in a specified spatial relationship occur in an image. The number of occurrences is then tabulated within a GLCM, from which a range of textural features may be calculated.

In this study, GLCM's were calculated using 64 gray levels and for the first and second pixels adjacent to a pixel of interest at all angles (horizontal, vertical, and diagonals). For each of the 1600-kHz sidescan sonar mosaics, the GLCM was calculated and a suite of textural features (e.g., Chak et al. 2020) assessed within sliding windows of 20×20 pixels (1 m^2). After visually inspecting these resulting raster layers, four GLCM texture features (energy, correlation, standard deviation, and kurtosis) were retained based on their ability to delineate cultch areas and cultch area boundaries effectively across each site (Fig. S4).

In addition, the image entropy (e.g., Gonzalez et al. 2011) within each sliding window was retained along with a version of the original sonar image that was smoothed using a 2D Gaussian kernel with a standard deviation of 3 pixels. These six raster layers, with the same pixel resolution ($0.05 \times 0.05 \text{ m}$) as the original sidescan mosaics, were used to classify areas of cultch using a convolutional neural network (Figs. S4, S5). The network was trained separately for each site and used to quantify the loss of habitat due to sediment burial.

Network Description and Training

U-net is a pixel-based fully convolutional neural network used for semantic segmentation. It has a symmetric architecture comprised of a down-sampling path that captures pixel context and an up-sampling path that propagates contextual information to higher-resolution layers for pixel localization (Ronneberger et al. 2015; Fig. S5). While most deep networks require large amounts of training data, this architecture has proven to be a powerful segmentation tool in scenarios with limited training examples. It has been used extensively for biomedical applications (e.g., Quo et al. 2018; Zyuzin et al. 2018; Guan et al. 2020), as well as in land-use classification studies that employ semantic segmentation on multispectral remote sensing imagery of urban and coastal environments (e.g., Li et al. 2018; Chu et al. 2019; Garg et al. 2019; Stoian et al. 2019). The importance of pixel context in the U-net framework, and its utility in scenarios with limited training data, is similarly applicable in sonar image segmentation. We used a modified version of U-net implemented in the MATLAB (v. 2018b) Deep Learning Toolbox for our reef classification problem, as outlined in the Supplementary Information (Fig. S5).

Labeled data for training and validation were obtained by manually classifying reef and non-reef pixels within image subsets, typically 1024×1024 pixels, that were extracted from the 1600-kHz sonar mosaics for each survey. Each labeled subset spanned reef and non-reef areas within the larger sonar mosaics. One or two labeled image subsets from both survey years were included for training to best represent the diversity of seabed characteristics and range of sonar artifacts within the mosaics (Table S1). To minimize inconsistencies in labeling, which might influence the performance of the network, all labeling was done by a single individual (O. Caretti) at a constant map scale using MATLAB's Image Labeler application. The high turbidity of the waters precluded using visual seabed survey techniques for additional validation.

Our primary goal was to determine temporal changes in the exposed area of reef substrate at each site using objective criteria. Therefore, a separate U-net model was trained for each site using labeled data and the texture feature layers calculated from both the 2016 and the 2018 surveys. This effort created network models that were specific to the type of cultch material used in each reef's construction and the local character of the surrounding seabed, and provided a systematic approach to quantifying changes in reef area within each site. The differences among sites and the number of available images did not support training a single, more generalized classification model. Key training parameters are summarized in the Supplementary Information.

Network Validation

Trained site-specific networks were validated using two $1024 \times 1024 \times 6$ (pixel \times pixel \times number of feature layers) labeled data subsets, one from each survey year, that were not used in training. The normalized confusion matrix was used to summarize the proportion of correctly and incorrectly labeled pixels for the reef and non-reef classes (Table 2). The normalization was based on the number of pixels mapped in each class, such that the values in cell [1, 2] represent errors of commission (non-reef pixels misclassified as reef) and values in cell [2, 1] represent errors of omission (reef pixels misclassified as non-reef). Commission errors were the largest at Jones Bay (0.140) and the largest errors of omission were observed at Bonner Bay (0.141), Caffee Bay (0.120), and Rose Bay (0.150) (Table 2). The Supplementary Information further documents the accuracy, intersection over union, and boundary F1 scores for these network models (Table S3).

Image Segmentation

To generate segmented images for each site's sonar mosaics, the six feature layer matrices for the entire map area were input into the appropriate site-specific trained network. The resulting binary (reef vs. non-reef) images were then

Table 2 Site-specific normalized confusion matrix, normalized by rows, or referenced to total number of mapped pixels in each class. Rows represent mapped classification and columns represent reference validation

Site	Mapped (predicted) class	Reference class	
		Reef	Non-reef
BB	Reef	0.921	0.079
	Non-reef	0.141	0.859
DC	Reef	0.916	0.084
	Non-reef	0.043	0.957
JB	Reef	0.860	0.140
	Non-reef	0.073	0.927
DB	Reef	0.908	0.092
	Non-reef	0.045	0.955
RB	Reef	0.964	0.036
	Non-reef	0.150	0.850
CB	Reef	0.956	0.044
	Non-reef	0.120	0.880

median-filtered using a 3×3 -pixel kernel and masked to a region of interest common to the 2016 and 2018 surveys. Eight-direction connectivity (horizontal, vertical, and diagonal directions) was used to link pixels and identify patches of reef material. Isolated patches smaller than 10×10 pixels (0.25 m^2) were masked before calculating mapped reef areas.

Characterization of Reef Seabed

Reef Geometry and Setting

Habitat metrics were calculated from the segmented images to describe initial reef characteristics, and then compared between surveys to describe changes in habitat over time. The area and perimeter of each reef patch, as defined based on pixel connectivity, were calculated and then summed across all patches in the segmented images. These summed values are referred to as the mapped area (A_m) and mapped perimeter (P_m) of the reef. The perimeter-area ratio was calculated to assess the patchiness of the reef habitats. Reef centroid was calculated by averaging the X and Y locations of all pixels classified as reef material.

The initial geometry of each reef was determined by finding the closed polygon boundary encapsulating the semi-contiguous portion, or footprint, of each reef. This boundary was calculated using an alpha-shape algorithm, which generates a non-convex bounding area around a set of unorganized points (i.e., reef pixels) with a specified fit (Edelsbrunner et al. 1983). The eccentricity, ratio of minor to major axes length for an ellipse fit to the reef-bounding polygon, was calculated for each reef, along with its circularity, which represents the ratio

of the polygon's area to the area of a circle with the same perimeter (Haralick 1974).

The slope of the substrate surrounding each reef was estimated by calculating the angle from the horizontal between the shallowest and deepest regions in the bathymetry maps. Distance and direction to the nearest shoreline were measured from the reef edge or corner closest to the surrounding marsh in ArcGIS Pro.

Local Relief

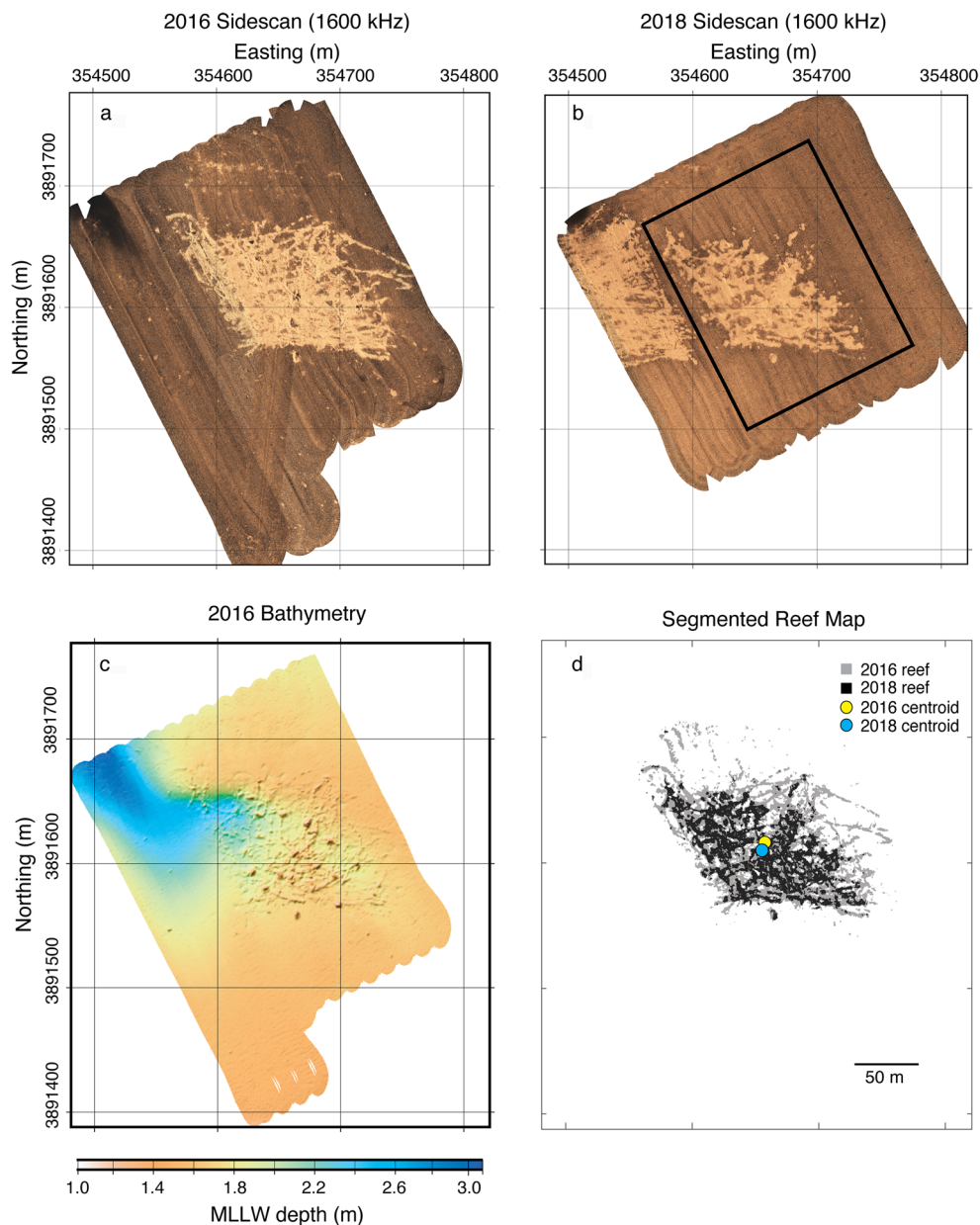
The relief of a reconstructed reef is important for preventing burial of oysters and ensuring that substrate is available for larval settlement (Lenihan 1999; Colden et al. 2017), as well as altering local hydrodynamic flow to reduce hypoxia and promote habitat quality (Lenihan and Peterson 1998; Lenihan 1999; Whitman and Reidenbach 2012; Colden et al. 2016). Local relief was calculated in a moving window with a 2-m radius ($\sim 12.5 \text{ m}^2$) around each central pixel in the bathymetric grid. This corresponds to the spatial scale of the largest cultch mounds constructed at Bonner Bay (Fig. 2c). These relief maps were then masked using the reef footprint polygon defined from segmentation of 2016 sonar imagery to identify whether local relief changed over time across a constant area. The median, 95% and 99% quantiles, and maximum local relief values were tabulated within this bounding polygon for each survey.

Adjusted Reef Area Estimates

The mapped reef areas (A_m) referenced above were adjusted to account for errors in the classification. Of the total area classified within a site-specific mask (A_t), the proportion (p_r) that is reef material can be calculated as $p_r = w_r f_{11} + w_n f_{21}$, where w_r is the proportion of the area that was mapped as reef ($w_r = A_m/A_t$) and w_n is the proportion of the area that was mapped as non-reef ($w_n = 1 - w_r$). The f_{11} term represents the proportion of the mapped reef area that was identified correctly (i.e., the [1,1] cell in each site's normalized confusion matrix; Table 2), and the f_{21} term represents the proportion of the mapped non-reef area that was reef (i.e., the omission error, or the [2,1] cell in each site's normalized confusion matrix; Table 2) (cf., Olofsson et al. 2013, 2014, 2020; Stehman 2013). The adjusted reef area (A_a) was calculated as $A_a = p_r A_t$.

Both the mapped (A_m) and adjusted (A_a) areas are listed in Table 3, along with the change in reef area between 2016 and 2018, calculated based on both the mapped and adjusted areas. Due to errors of omission, adjusted area estimates were typically larger than mapped area estimates, with the exception of the Deep Bay and Ditch Creek reefs, where the adjusted values were slightly smaller in 2016. This result is consistent with those reported in many land classification studies (e.g., Olofsson et al. 2013, 2014). The percentage change in reef

Fig. 2 Bonner Bay (a) 2016 and (b) 2018 sidescan sonar mosaics (0.05-m pixel resolution), (c) 2016 bathymetry map (0.5-m resolution grid), and (d) map of 2018 segmented reef pixels (black) overlain on 2016 segmented reef pixels (gray). Reef centroid marked for each year in d. Study reef highlighted in b. Northings and eastings are for UTM Zone 18



area calculated from adjusted area estimates (ΔA_a) was consistently lower than the mapped area changes (ΔA_m) (Table 3).

Reef Habitat Function

The density of live oysters was measured on each reef to confirm whether the reefs constructed by the NC DMF functioned as habitat for oysters, and whether their function as habitat changed as the exposed reef area changed over time. Immediately after mapping in August 2016, four oyster settlement trays (0.25 m²) were deployed on each reef, filled with cultch unique to each reef (Table 1), and were placed flush against the reef surface. The oyster trays were used to provide a relative measure of oyster recruitment, as well as sub-adult

and adult densities, while standardizing the amount of material within trays and among replicates. Trays were sampled by SCUBA divers once every 2–3 months from October 2016 to October 2018, and the number of live oysters were counted. All material was returned to the trays after each sampling event.

Results

Characteristics of Constructed Reefs

All reefs were built within 100–200 m of the nearest saltmarsh edge (Table 4). Bonner Bay, Ditch Creek, and Deep Bay were

Table 3 Two-dimensional reef habitat characteristics calculated from segmented images. Mapped reef area (A_m) is the sum of pixel areas classified as reef. Adjusted reef area (A_a) accounts for errors in classification. Change in reef centroid lists distance and direction of translation between 2016 and 2018 surveys

Site	Year	A_m mapped area (m ²)	A_a adjusted area (m ²)	ΔA_m (%)	ΔA_a (%)	P_m (m)	$P_m:A_m$	Δ Reef centroid
BB	2016	10,531	12,138	-52	-35	3544	0.34	6.5 m SW
	2018	5034	7849			2863	0.57	
DC	2016	7872	7742	-73	-65	1931	0.25	24.2 m SW
	2018	2146	2743			1590	0.74	
JB	2016	2859	3172	-66	-47	3351	1.17	2.8 m E
	2018	974	1689			1380	1.42	
DB	2016	6086	5951	-33	-29	943	0.16	5.5 m NE
	2018	4106	4240			965	0.24	
RB	2016	9061	10,095	-25	-18	1562	0.17	7.5 m NW
	2018	6829	8277			1025	0.15	
CB	2016	8710	9610	-24	-18	1661	0.19	5.5 m NE
	2018	6595	7843			2284	0.35	

generally bordered by saltmarsh along their southern edges. Marshes bordered Caffee and Jones Bays to the north, and Rose Bay to the east (Fig. 1; Table 4). The shorelines surrounding the reefs were unmodified, natural saltmarsh. All reefs were built on relatively flat surfaces, with Bonner Bay and Ditch Creek on the steepest slope of 0.35° (Table 4).

When mapped after their construction in August 2016, reefs were generally rectilinear in shape, with circularities <0.4 and eccentricity values >0.6 (Table 4; Figs. 2, 3, 4, 5, 6, 7a). Ditch Creek was the most elongated and narrow (Fig. 3a), and Deep and Rose Bays were the most square-shaped reefs (Fig. 5a and 6a; Table 4).

Reefs were constructed by spreading cultch to create an area of mostly contiguous substrate, with the exception of Jones Bay. The Jones Bay reef was built as a series of discontinuous ridges and had a perimeter-area ratio ~3.5 times that of any other reef (Fig. 4; Table 3). Bonner Bay was the largest reef ($A_a = 12,138 \text{ m}^2$), followed by Rose Bay, Caffee Bay, Ditch Creek, Deep Bay, and Jones Bay ($A_a = 3172 \text{ m}^2$) (Table 3).

Table 4 Initial 2016 reef characteristics. Average thickness of cultch was calculated using material volumes (Table 1) and the mapped (A_m) and adjusted (A_a) area estimates (Table 3). Characteristics of the reef

Site	Avg. depth (m)	Substrate slope	Distance (m) and direction (°) to shore	Avg. cultch thickness (cm) from $A_m A_a$	Reef footprint characteristics			
					Area (m ²)	Perimeter (m)	Circularity	Eccentricity
BB	1.7	0.33° NW	183 m, 176°	9.1 7.9	11,955	1307	0.09	0.82
DC	1.5	0.35° NW	162 m, 139°	5.0 5.1	9096	599	0.32	0.98
JB	1.4	0.17° SE	127 m, 336°	9.2 8.3	5570	408	0.42	0.81
DB	2.8	0.20° N	211 m, 165°	7.7 7.9	6376	485	0.34	0.69
RB	2.3	0.16° SW	155 m, 114°	6.4 5.7	9624	896	0.15	0.61
CB	1.7	0.20° S	121 m, 312°	7.3 6.6	9950	847	0.17	0.80

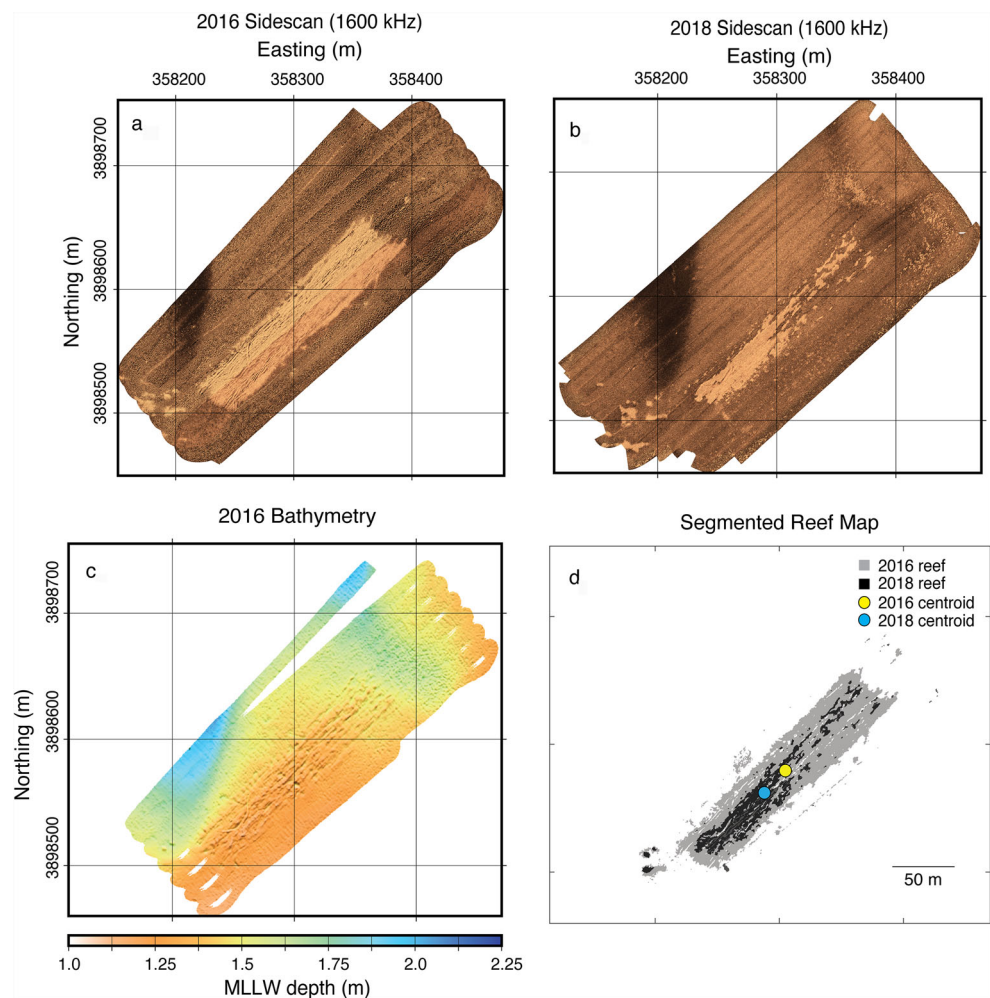
Substrates at all reefs were constructed with low local relief, <0.3 m at the 95% quantile level (Figs. 2, 3, 4, 5, 6, 7c; Table 5). At Bonner Bay, roughly a dozen small mounds were created with maximum heights of 0.5–0.75 m (Fig. 2c; Table 5). Low-relief (<0.4 m) ridges were formed at the other sites (Figs. 3, 4, 5, 6, 7c). The average thickness of cultch, calculated from the adjusted area and volume of material reported by the NC DMF (Table 1), ranged from ~5 cm at Ditch Creek to ~8 cm at Bonner, Jones, and Deep Bays (Table 4).

Changes in Reef Characteristics Over Time

As portions of cultch were covered with sediment, these areas became acoustically indistinguishable from the surrounding sedimented substrate. These changes are evident in panels a and b in Figs. 2, 3, 4, 5, 6, and 7, which display sonar mosaics for the August 2016 and May 2018 surveys. These changes were identified in the sidescan image-based and GLCM-textural features used in the classification, and the resulting

footprint (initial area, perimeter, circularity, and eccentricity) are defined by the bounding polygon for the semi-contiguous reef area

Fig. 3 Ditch Creek (a) 2016 and (b) 2018 sidescan sonar mosaics (0.05-m pixel resolution), (c) 2016 bathymetry map (0.5-m resolution grid), and (d) map of 2018 segmented reef pixels (black) overlain on 2016 segmented reef pixels (gray). Reef centroid marked for each year in d. Northings and eastings are for UTM Zone 18



segmented images (Figs. 2, 3, 4, 5, 6, 7d) highlight the loss of restored cultch substrate at each site over the 21-month period.

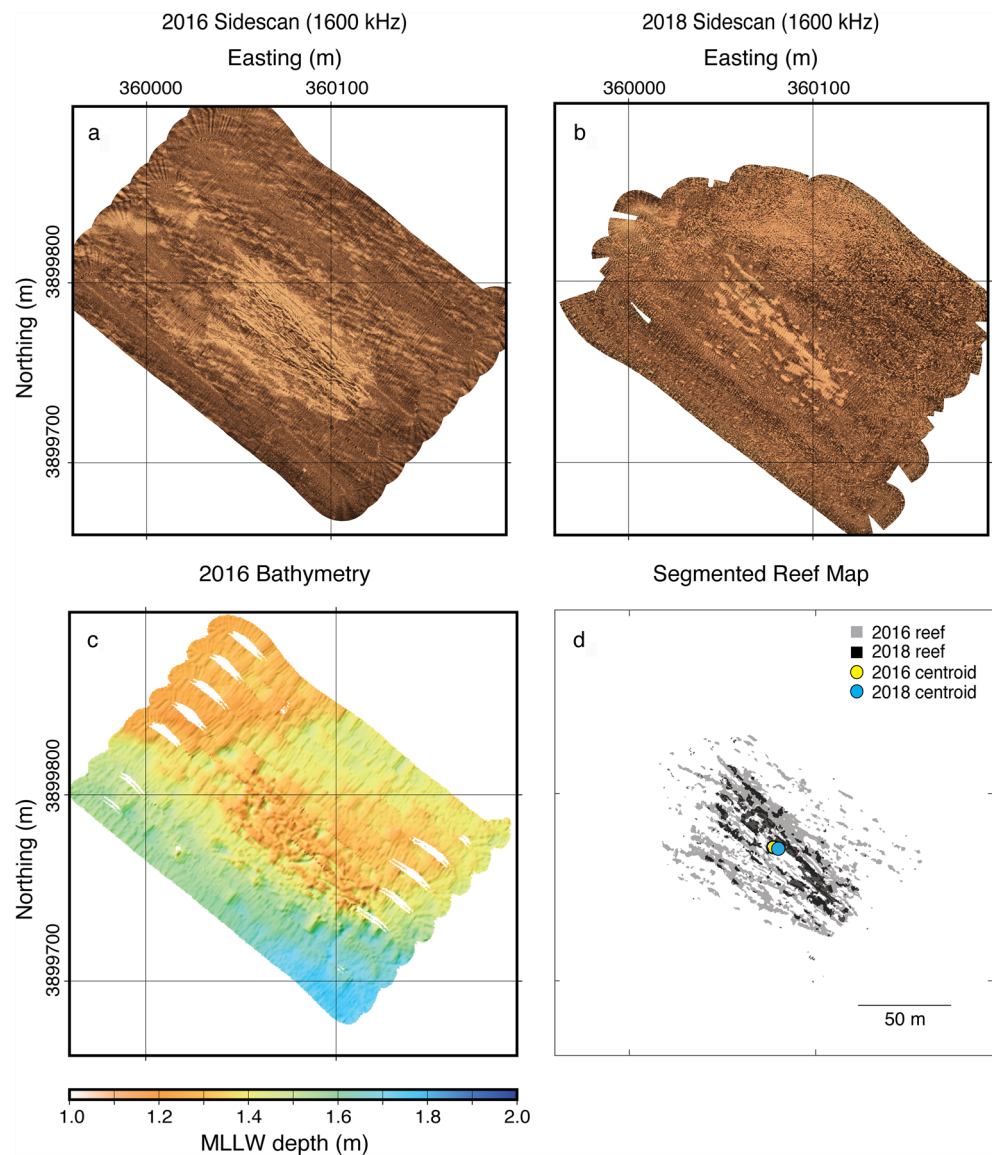
The Ditch Creek and Jones Bay reefs, both located within Jones Bay, suffered the greatest burial of cultch substrate (Figs. 3 and 4), with decreases of 65% and 47% in adjusted reef area, respectively (Table 3). The Jones Bay reef, which had the smallest original area and the greatest perimeter-area ratio, retained an adjusted area of just 1689 m², and its perimeter-area ratio increased from 1.17 to 1.42. The originally mid-sized Ditch Creek reef decreased in size to an adjusted area of 2743 m² and its perimeter-area ratio tripled to 0.75. Sidescan sonar imagery collected in 2018 showed the highly fragmented nature of the Jones Bay reef (Fig. 4b and 4d), and that sediment burial occurred chiefly across the northern half of the Ditch Creek reef (Fig. 3b and 3d; Table 3).

The largest site, which was constructed within Bonner Bay along the Bay River, was intermediately impacted by sedimentation (Fig. 2). When mapped in 2018, 35% of its original substrate had been sedimented, leaving an estimated adjusted area of 7849 m². Its perimeter-area ratio increased from 0.34 to 0.57. The lost substrate was primarily along its eastern and

northern margins, and included several narrow bands of cultch that extended away from the main reef area, as well as areas of low local relief between mounds (Fig. 2b and 2d). In 2017, the NC DMF constructed additional habitat to the west of the 2016 reef. Although its original footprint is unknown, large sections of this low-relief cultch substrate remained exposed when surveyed in May 2018 (Fig. 2b).

The Deep Bay reef, positioned north of the Pamlico River, lost 29% of its adjusted area (Fig. 5). Much of this loss was along the margins of the reef, and from an area extending to the southwest that appeared, based on the texture and intensity of the sonar imagery, to be more sparsely covered with cultch than the central portions of the reef (Fig. 5a and 5b). When mapped in 2018, the adjusted area of cultch substrate at Deep Bay was 4240 m². The perimeter-area ratio increased from 0.16 to 0.24, but remained low relative to the more patchy southern reefs (Table 3). The Deep Bay habitat constructed in 2016 was located <40 m west of a section of low-relief reef built in 2015 (Fig. 5). Although the original footprint of this reef is unknown, significant cultch substrate remained exposed in 2018, nearly 3 years after its construction (Fig. 5b).

Fig. 4 Jones Bay (a) 2016 and (b) 2018 sidescan sonar mosaics (0.05-m pixel resolution), (c) 2016 bathymetry map (0.5-m resolution grid), and (d) map of 2018 segmented reef pixels (black) overlain on 2016 segmented reef pixels (gray). Reef centroid marked for each year in d. Northings and eastings are for UTM Zone 18. Artifacts in bathymetric data reflect sea state during the survey



The nearby Rose Bay (Fig. 6) and Caffee Bay (Fig. 7) reefs both lost 18% of their adjusted areas, retaining areas of 8277 m² and 7843 m², respectively (Table 3). As with Deep Bay, the loss of cultch was concentrated along the margins and among areas of the reef that appeared more sparsely covered when first surveyed in 2016. The perimeter-area ratios remained low for these reefs, being essentially unchanged at Rose Bay (0.17 vs. 0.15) and almost doubling (0.19 vs. 0.35) at Caffee Bay (Table 3).

Because the penetration depth of very high-frequency sonars is negligible within these sediments (Huff 2008; Feldens et al. 2018), burial depths on the order of ~1 cm may be sufficient to explain the observed decrease in sidescan amplitude. Uncertainties in vehicle positioning and sea surface height unfortunately preclude the direct measurement of sediment thickness based on changes in the elevation of the seabed. However, maps comparing the 2016 and 2018 bathymetry are displayed

in the Supplementary Information. Profiles crossing the Ditch Creek ($\Delta A_a = -65\%$, Fig. S6), Bonner Bay ($\Delta A_a = -35\%$, Fig. S7), and Caffee Bay ($\Delta A_a = -18\%$, Fig. S8) reefs demonstrate that sediments largely blanketed the underlying cultch, with no indication of widespread sinking or lateral spreading of material. The maximum change in local relief between the 2016 and 2018 surveys indicates that the burial depth can be locally no more than 10 cm (Table 5).

Reef Habitat Function

Settlement and the subsequent survival of oysters occurred on all reefs, suggesting that they functioned as habitat for oysters in some capacity (Fig. 8). Reefs that lost less area to sediment burial (Deep Bay, Rose Bay, and Caffee Bay) consistently had more oysters than the reefs that became most heavily sedimented (Jones Bay and Ditch Creek) (Fig. 8). There were

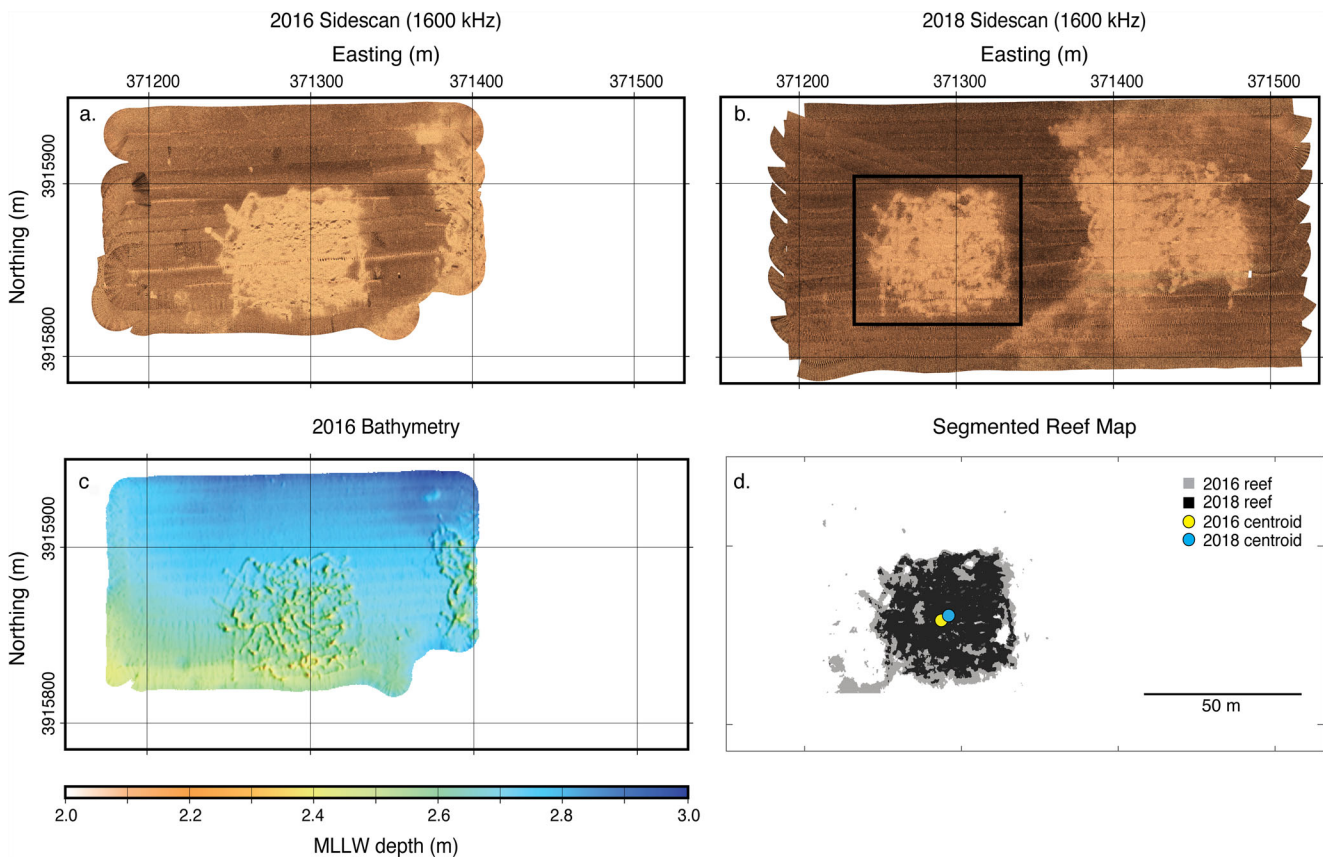


Fig. 5 Deep Bay (a) 2016 and (b) 2018 sidescan sonar mosaics (0.05-m pixel resolution), (c) 2016 bathymetry map (0.5-m resolution grid), and (d) map of 2018 segmented reef pixels (black) overlain on 2016

segmented reef pixels (gray). Reef centroid marked for each year in d. Study reef outlined in b. Northings and eastings are for UTM Zone 18

several instances where some oyster settlement trays at Jones Bay and Ditch Creek were buried in ~3–5 cm of sediment, and no live oysters were recorded in the buried trays. Among the reefs with the largest areas in May 2018, Caffee Bay and Rose Bay exhibited a rise in average oyster density that extended through October. At Bonner Bay, where more reef area had been lost, oyster density dropped substantially by August 2018, indicating that oyster mortality at this reef outpaced recruitment (Table 3; Fig. 8).

Discussion

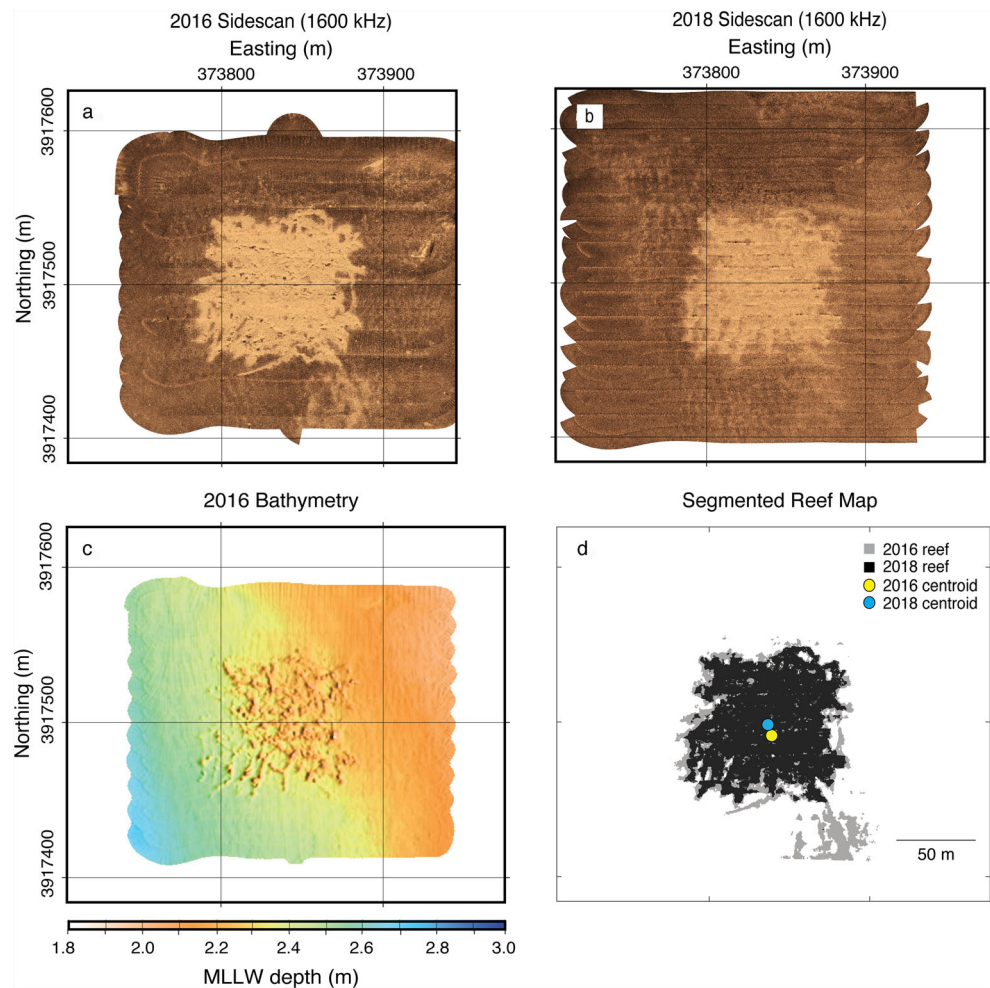
In the summer of 2016, six low-relief oyster cultch reefs were constructed by the NC DMF within southwestern Pamlico Sound. To minimize the potential for reef subsidence, or sinking of the cultch into the sediments (e.g., Stokes et al. 2012; Grizzle and Ward 2016), these reefs were principally located on relatively hard sedimented bottom areas, as assessed using sounding pole refusal data (NC DMF 2020b). High-resolution sidescan sonar and bathymetric data were collected a few weeks after construction in August 2016, and the reefs were mapped again in May 2018. As with other subtidal reefs in

North Carolina and Virginia (e.g., Lenihan 1999; Powers et al. 2009; Schulte et al. 2009; Colden and Lipcius 2015; Colden et al. 2016, 2017), the burial of restored substrate by sediments appears to limit their short-term success—with the reefs in Pamlico Sound losing 18–65% of their original area over this 21-month period. Nonetheless, contiguous areas of very low-relief (<0.3 m) substrate persisted on some reefs and functioned as habitat for the settlement and growth of oysters. The susceptibility of restored oyster cultch reefs to habitat loss depended on the local sediment supply and hydrodynamics within each sub-basin.

Importance of Location when Siting Oyster Restoration

The reefs monitored in this study were located in sub-bays near the confluence of the Bay, Neuse, and Tar-Pamlico riverine estuaries. The path of fine-grained sediment through this system typically involves repeated deposition and local transport following wind-induced resuspension (Wells and Kim 1989; Giffin and Corbett 2003), with elevated suspended sediment loads likely during the period of high discharge and turbidity following Hurricane Mathew. Ditch Creek likely supplies additional

Fig. 6 Rose Bay (a) 2016 and (b) 2018 sidescan sonar mosaics (0.05-m pixel resolution), (c) 2016 bathymetry map (0.5-m resolution grid), and (d) map of 2018 segmented reef pixels (black) overlain on 2016 segmented reef pixels (gray). Reef centroid marked for each year in d. Northings and eastings are for UTM Zone 18



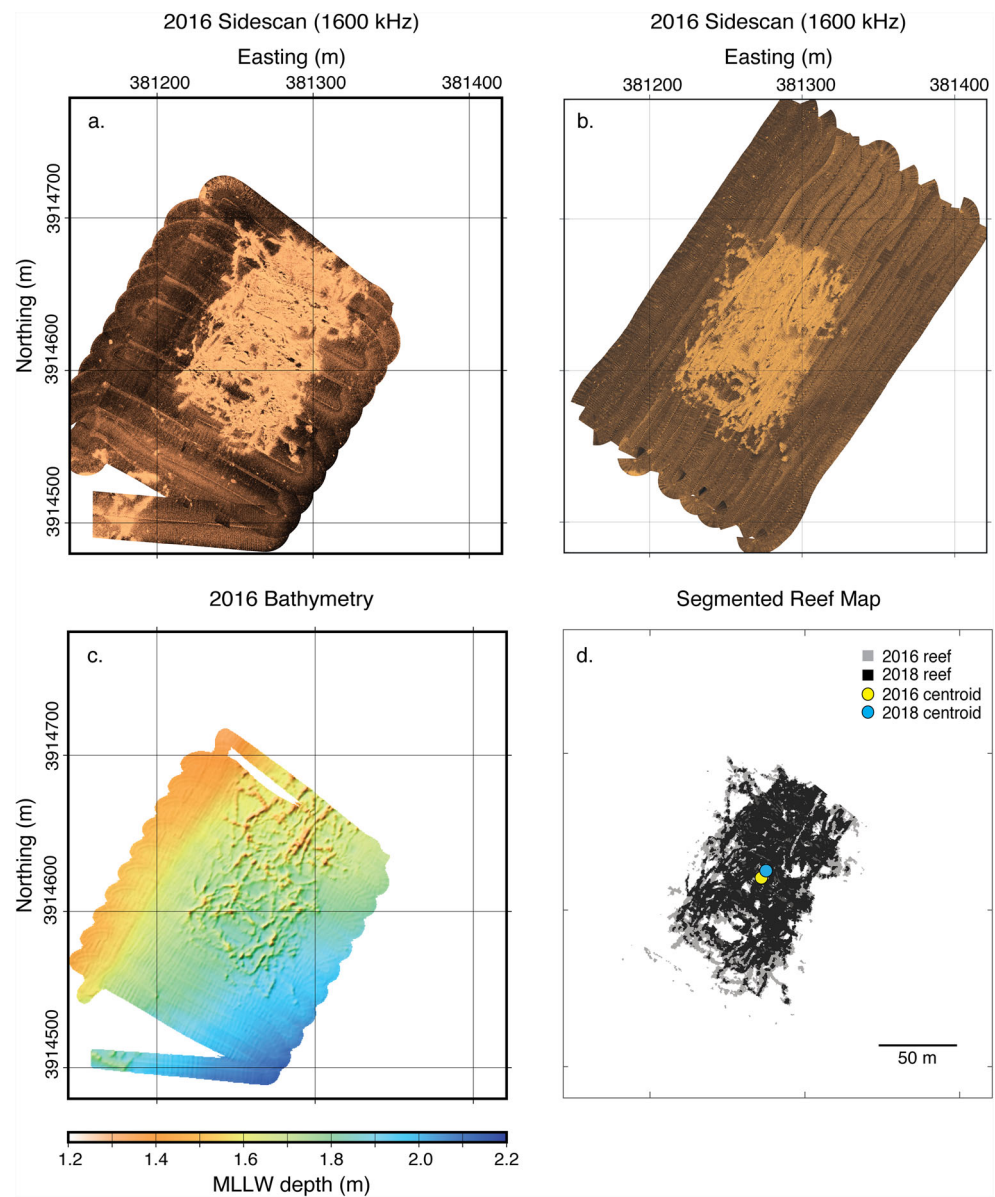
sediment to the reef built near its mouth, and local sediment delivery at Bonner Bay is enhanced by its proximity to three small drainages (Fig. 1c). Fine-grained sediment may also be supplied to reefs by erosion of nearby marsh shorelines, which is heavily influenced by shoreline orientation and local fetch (Eulie et al. 2017). Northern facing shorelines adjacent to Ditch Creek, Bonner Bay, and Deep Bay likely experienced higher rates of erosion than reefs adjacent to southern facing shorelines, as the strongest winds during our study occurred from the north, particularly during the passage of Hurricane Mathew.

Bottom water turbidity measurements in the Neuse and Pamlico River estuaries have shown that passing atmospheric fronts generating rapidly shifting wind directions and speeds in excess of 4 m s^{-1} provide sufficient wave energy to resuspend bottom sediments within this shallow basin (Giffin and Corbett 2003). Large turbidity events occurred mostly as the result of northwesterly and northeasterly winds, which are typically associated with the highest wind speeds (Giffin and Corbett 2003). Winds in Pamlico Sound frequently exceeded 4 m s^{-1} during our study, which suggests that turbidity events, and/or the activation of bottom sediments, were common between mapping surveys.

Hydrodynamic models (Xie and Eggleston 1999; Jia and Li 2012a, b) suggest that northerly winds drive water movement into bays and rivers at depth along the western margin of Pamlico Sound. We hypothesize that these hydrodynamic conditions would locally transport resuspended sediments toward reefs in Jones Bay and the Bay River, and into the Pamlico River and away from northern reefs, which is supported by the greater extent of burial documented at southern reefs. The most heavily impacted reefs, Jones Bay and Ditch Creek, were constructed along the middle section of the east-west trending Jones Bay (Fig. 1c). Sediments deposited on the Jones Bay and Ditch Creek reefs were coarser (i.e., more sandy) than sediments deposited at the other reefs (O. Caretti personal obs.). The extremely shallow depths surrounding the Jones Bay reefs (1.5 m), combined with its exposure to wind and wave energy, would have supported the resuspension and transport of this coarser material locally within the bay (Fig. 9a).

The reefs constructed north of the Pamlico River experienced lower-energy hydrodynamic conditions (Jia and Li 2012a, b) and had fewer potential sediment sources (rivers, marsh creeks, and shorelines susceptible to erosion) and were

Fig. 7 Caffee Bay (a) 2016 and (b) 2018 sidescan sonar mosaics (0.05-m pixel resolution), (c) 2016 bathymetry map (0.5-m resolution grid), and (d) map of 2018 segmented reef pixels (black) overlain on 2016 segmented reef pixels (gray). Reef centroid marked for each year in d. Northings and eastings are for UTM Zone 18



the least impacted by sedimentation (Fig. 9b). Sediment burial at these reefs occurred primarily along their sloping margins, and across areas where the intensity and texture of the 2016 imagery suggests a somewhat lower density of cultch on the seabed. Preferential burial of the reef edges is consistent with earlier observations on restored reefs in the Neuse River estuary (Lenihan 1999) and Chesapeake Bay (Colden et al. 2016, 2017).

Several studies have suggested that reef success can be linked to their initial height (Lenihan 1999; Colden et al. 2016, 2017; Lueck et al. 2019). Taller reefs may naturally encounter faster currents (e.g., Lueck et al. 2019). They also induce a hydrodynamic response whereby water passing over them must flow faster, to preserve continuity of energy, relative to water flowing at a similar depth adjacent to the reef (Lenihan 1999). Bed roughness also tends to increase with

reef height (Styles 2015; Colden et al. 2017), leading to higher turbulent stress and mixing within the overlying water column (Reidenbach et al. 2010; Styles 2015). These higher velocities and shear stresses inhibit the local deposition of fine-grained sediments compared to lower relief reefs. On patchy reefs, such as the Jones Bay reef or among the mounds at Bonner Bay, turbulent flow may weaken at the transition between rough (reef) and smoother (sediment) surfaces, which may promote deposition.

Similarly, the strength of turbulent flow may vary between natural and restored reefs, or conceivably between sites constructed from different cultch materials, that differ in bed roughness (e.g., Whitman and Reidenbach 2012). Bed roughness may have increased on reefs with higher total oyster densities as oysters continued to settle, survive, and grow on reefs with less burial. This could initiate a positive feedback

Table 5 Median, 95% and 99% quantiles, and maximum local reef relief (m) calculated within a moving 2-m radius (12.5 m² area). Quantiles were determined using all pixels within the reef-bounding polygon calculated from the 2016 segmented images

Site	Year	Median	95% quantile	99% quantile	Maximum
BB	2016	0.09	0.28	0.50	0.74
	2018	0.08	0.25	0.41	0.64
DC	2016	0.06	0.17	0.17	0.28
	2018	0.05	0.12	0.16	0.21
JB	2016	0.09	0.22	0.22	0.30
	2018	0.05	0.12	0.15	0.19
DB	2016	0.10	0.29	0.29	0.35
	2018	0.11	0.21	0.25	0.32
RB	2016	0.07	0.20	0.26	0.43
	2018	0.10	0.21	0.26	0.34
CB	2016	0.09	0.22	0.30	0.40
	2018	0.12	0.24	0.30	0.40

whereby further burial was limited, and more substrate for oyster settlement was available relative to reefs with fewer oysters.

In lower-energy environments, the persistence of reefs within Chesapeake Bay displayed a threshold response, with reefs taller than 0.3 m surviving, and those with less relief being buried by sediment (Colden et al. 2017). The reefs constructed in 2016 in Pamlico Sound all had <0.3 m of local relief across 95% of their substrate areas, putting them at risk of burial. Although portions of the four reefs in lower-energy hydrodynamic settings were lost, significant (~4000–8000 m²) contiguous sections persisted after 21 months such that

65–80% of their original areas remained exposed and available for larval settlement. Oyster settlement was consistently higher on these reefs and continued through October 2018, with the exception of Bonner Bay, which suggests that reefs in Deep Bay, Caffee Bay, and Rose Bay may persist and provide suitable oyster habitat in the short term. Moreover, sidescan imagery shows that the cultch substrate restored in 2015 in Deep Bay (adjacent to the 2016 reef) remained unburied ~3 years after its construction. The exposure of contiguous cultch substrates over multi-year periods demonstrates that low-relief reefs can persist longer than suggested by some earlier studies (e.g., Lenihan 1999; Colden et al. 2017), provided they are in settings with a low potential for sediment deposition.

The moderate to extensive burial observed for some reefs in Pamlico Sound reduces the available substrate for settling oyster larvae, lowers the likelihood that oysters will be able to grow to harvestable size, and limits the long-term ecosystem benefits of the restoration effort (Lenihan 1999; Powers et al. 2009; Colden and Lipcius 2015; Colden et al. 2017). In a dynamic, wind-driven system like Pamlico Sound, reef burial may be ephemeral; however, even if episodes of burial are short-lived, it is unlikely that such reefs will provide suitable habitat to establish and sustain a healthy reef community.

Recommendations and Conclusions

The loss of restored oyster cultch reefs in western Pamlico Sound was driven primarily by sediment burial, which varied spatially based on local sediment dynamics. While the loss of viable reef area to sediment burial is not necessarily a new finding, the variation in burial among reefs seen in this study

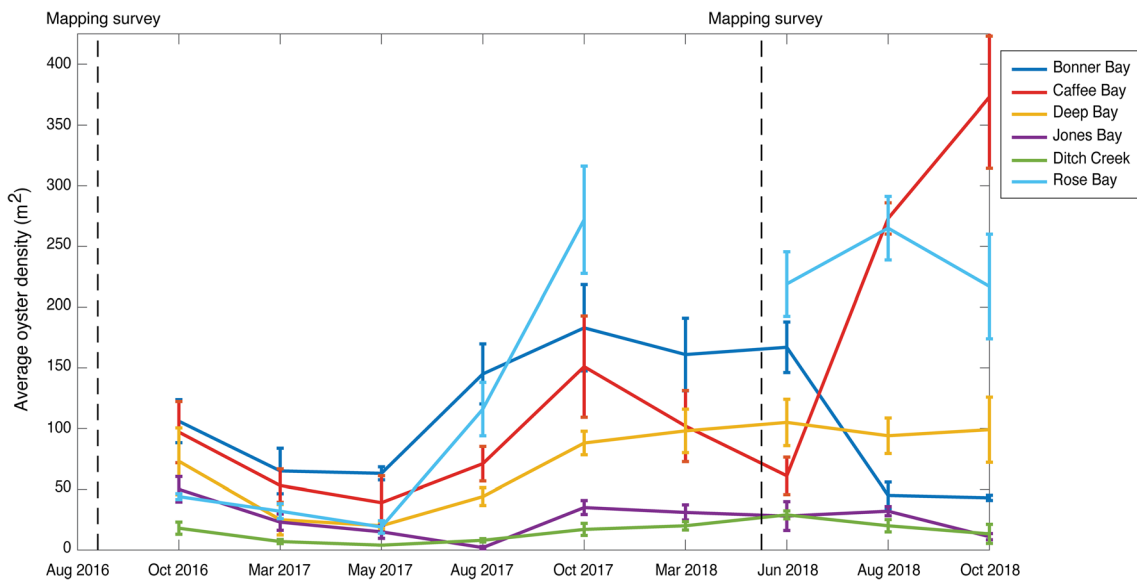


Fig. 8 Mean oyster density and standard error (vertical bar) collected from oyster settlement trays (*n* = 4) and sampled repeatedly over time. Vertical dashed lines indicate dates of mapping surveys

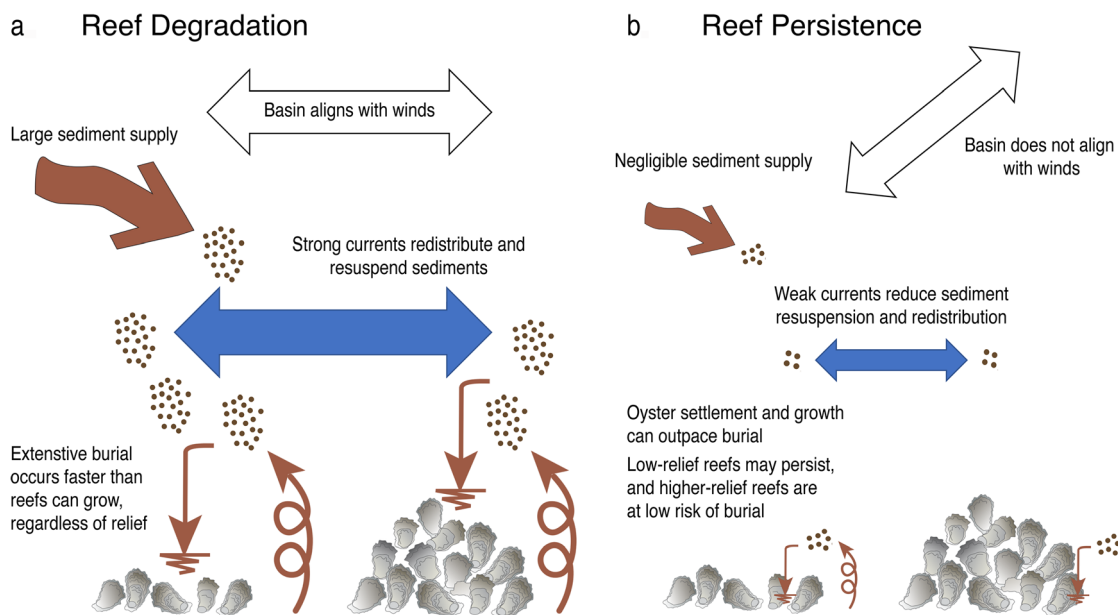


Fig. 9 Mechanisms driving (a) degradation or (b) persistence of restored reefs in southwestern Pamlico Sound. (a) Southern reefs (JB, DC, and BB) experienced a large sediment supply and strong hydrodynamic conditions that promoted movement of benthic sediments and caused reef burial. Initial reef characteristics and oyster settlement and growth

were not robust enough to overcome sediment deposition. (b) Northern reefs (DB, RB, and CB) had fewer potential sediment sources, experienced lower-energy hydrodynamic conditions, and were least impacted by sedimentation. Low-relief reefs persisted, with sediment primarily deposited along reef margins

underscores that restoration efforts should consider fine-scale sediment dynamics as a key factor in site selection, especially in shallow, wind-driven estuarine systems. This may require in situ monitoring prior to construction, coupled with regional-scale to local-scale modeling of sediment dynamics to identify areas at high risk of burial and areas that would be more suitable for restoration (e.g., Liu and Huang 2009; Xue et al. 2012; Zang et al. 2017). Existing habitat suitability index (HSI) models (e.g., Pollack et al. 2012; Theuerkauf and Lipcius 2016; Puckett et al. 2018; Theuerkauf et al. 2019) should incorporate additional layers that identify the proximity of potential sediment sources (e.g., marsh creeks and larger rivers, actively eroding shorelines). Although not investigated in this study, high-resolution sediment sampling and grain size analysis within targeted basins would help predict the risk of sediment resuspension and deposition given predominant hydrodynamic conditions, and could be used as an additional predictor of habitat suitability. These layers will be crucial to incorporate in the development of a new HSI model for cultch oyster reef restoration in Pamlico Sound and similar turbid, shallow, wind-driven estuaries.

When constructed in low-energy environments, low-relief (<0.3 m) cultch substrates may persist for at least a few years; however, substrates of similar height are likely to be buried (at least ephemerally) in higher-energy settings (Fig. 9). Taller reefs may be less susceptible to loss through burial (Lenihan 1999; Colden et al. 2017), such that restoration designs that incorporate greater relief throughout the reef area may extend the percentage and longevity of substrate that remains exposed.

As all reefs exhibited sedimentation along their margins (Lenihan 1999; Colden et al. 2016, 2017; this study), designs with larger contiguous footprints and smaller perimeter-area ratios also may have greater longevity.

As shown here, repeated sonar and bathymetric mapping of restored oyster reefs allowed us to characterize the area, geometry, and structural complexity of restored habitats, and to monitor changes in these characteristics over time. A U-net convolutional neural network architecture was used to classify pixels within the sidescan sonar imagery using image-based and image-texture features calculated from gray-level co-occurrence matrices. This approach provided an objective way to identify reef substrate and make estimates of reef area that considered errors of omission and commission at each site, as well as appropriate resolution for fine-scale comparisons within and among reefs that, to our knowledge, has not yet been achieved.

The loss of reef area due to sedimentation can have cascading impacts on habitat quality for oysters, as well as the numerous ecosystem services provided by restored reefs. Previous studies have described many of the key considerations and factors that should be included in oyster restoration design to promote restoration success (e.g., Pollack et al. 2012; Lipcius et al. 2015; Puckett et al. 2018). This study contributes to that growing body of information by emphasizing the importance of reef location within the seascape, and shows that local sediment dynamics strongly impact reef persistence. This study and the questions it generated with respect to sediment transport processes are key to developing a robust

habitat suitability modeling framework for this type of oyster reef restoration.

Supplementary Information The online version contains supplementary material available at <https://doi.org/10.1007/s12237-021-00921-6>.

Acknowledgements We thank R. Patrick Lyon and Gina Long for assisting in data collection, Chris Norcross and Clara Frickmann for their efforts in processing the sidescan sonar and bathymetric datasets, and Shannon Ricci for discussions regarding the machine learning methodology. Jason Peters and staff at the North Carolina Division of Marine Fisheries provided valuable information on cultch reef construction and assisted with selecting study reefs for mapping and monitoring. Thanks to Geoff Douglas and the team at SeaRobotics Corporation for their assistance in developing the unmanned surface vehicle. We thank S. Simenstad and three anonymous reviewers for suggestions and comments that improved the manuscript.

Funding Funding for this project was provided by the North Carolina Department of Environmental Quality, Coastal and Recreational Fishing License Grant Program (2017-H-063) and the North Carolina Sea Grant Core Funding Program (R18-HCE-2). The acquisition of the unmanned surface vehicle and sonar was supported by the National Science Foundation (DBI-1522489). Computational resources were provided through the NVIDIA GPU Academic Grant program. Olivia Caretti received additional support from a National Science Foundation Graduate Research Fellowship.

References

- Baggett, L.P., S.P. Powers, R.D. Brumbaugh, L.D. Coen, B.M. DeAngelis, J.K. Greene, B.T. Hancock, S.M. Morlock, B.L. Allen, D.L. Breitburg, D. Bushek, J.H. Grabowski, R.E. Grizzle, E.D. Grosholz, M.K. La Peyre, M.W. Luckenbach, K.A. McGraw, M.F. Piehler, S.R. Westby, and P.S.E. Zu Ermgassen. 2015. Guidelines for evaluating performance of oyster habitat restoration. *Restoration Ecology* 23 (6): 737–745. <https://doi.org/10.1111/rec.12262>.
- Beck, M.W., R.D. Brumbaugh, L. Airoidi, A. Carranza, L.D. Coen, C. Crawford, O. Defeo, G.J. Edgar, B. Hancock, M.C. Kay, H.S. Lenihan, M.W. Luckenbach, C.L. Toropova, G. Zhang, and X. Guo. 2011. Oyster reefs at risk and recommendations for conservation, restoration, and management. *BioScience* 61 (2): 107–116. <https://doi.org/10.1525/bio.2011.61.2.5>.
- Blondel, P., L.M. Parson, and V. Robigou. 1998. TexAn: textural analysis of sidescan sonar imagery and generic seafloor characterization. *Oceans Conference Record (IEEE)* 1 (2): 419–423. <https://doi.org/10.1121/1.425676>.
- Burkholder, J., D. Eggleston, H. Glasgow, C. Brownie, R. Reed, G. Melia, C. Kinder, G. Janowitz, R. Corbett, M. Posey, T. Alphin, D. Toms, and N. Deamer. 2004. Comparative impacts of major hurricanes on the Neuse River and western Pamlico Sound ecosystems. *Proceedings of the National Academy of Sciences* 101 (25): 9291–9296.
- Callihan, R., B. Depro, D. Lapidus, T. Sartwell, and C. Viator. 2016. *Economic analysis of the costs and benefits of restoration and enhancement of shellfish habitat and oyster propagation in North Carolina*. Final Report to Albemarle-Pamlico National Estuary Partnership.
- Caress, D.W., and D.N. Chayes. 1995. New software for processing sidescan data from sidescan-capable multibeam sonars. *Oceans Conference Record (IEEE)* 1: 997–1000. <https://doi.org/10.1109/oceans.1995.528558>.
- Chak, P., P. Navadiya, B. Parikh, and K.C. Pathak. 2020. Neural network and SVM based kidney stone based medical image classification. *In Communications in Computer and Information Science* 1147: 158–173. https://doi.org/10.1007/978-981-15-4015-8_14.
- Chu, Z., T. Tian, R. Feng, and L. Wang. 2019. Sea-land segmentation with Res-UNet and fully connected CRF. *IGARSS 2019 - 2019 IEEE International Geoscience and Remote Sensing Symposium*: 3840–3843. <https://doi.org/10.1109/IGARSS.2019.8900625>.
- Clunies, G.J., R.P. Mulligan, D.J. Mallinson, and J.P. Walsh. 2017. Modeling hydrodynamics of large lagoons: insights from the Albemarle-Pamlico Estuarine System. *Estuarine, Coastal and Shelf Science* 189: 90–103. <https://doi.org/10.1016/j.ecss.2017.03.012>.
- Coen, L.D., R.D. Brumbaugh, D. Bushek, R. Grizzle, M.W. Luckenbach, M.H. Posey, S.P. Powers, and S.G. Tolley. 2007. Ecosystem services related to oyster restoration. *Marine Ecology Progress Series* 341: 303–307. <https://doi.org/10.3354/meps341299>.
- Colden, A.M., and R.N. Lipcius. 2015. Lethal and sublethal effects of sediment burial on the eastern oyster *Crassostrea virginica*. *Marine Ecology Progress Series* 527: 105–117. <https://doi.org/10.3354/meps11244>.
- Colden, A.M., K.A. Fall, G.M. Cartwright, and C.T. Friedrichs. 2016. Sediment suspension and deposition across restored oyster reefs of varying orientation to flow: implications for restoration. *Estuaries and Coasts* 39 (5): 1435–1448. <https://doi.org/10.1007/s12237-016-0096-y>.
- Colden, A.M., R.J. Latour, and R.N. Lipcius. 2017. Reef height drives threshold dynamics of restored oyster reefs. *Marine Ecology Progress Series* 582: 1–13. <https://doi.org/10.3354/meps12362>.
- Cowart, L., D.R. Corbett, and J.P. Walsh. 2011. Shoreline change along sheltered coastlines: insights from the Neuse River Estuary, NC, USA. *Remote Sensing* 3 (7): 1516–1534. <https://doi.org/10.3390/rs3071516>.
- Deaton, A.S., W.S. Chappell, K. Hart, J. O'Neal, and B. Boutin. 2010. *North Carolina coastal habitat protection plan*. North Carolina Department of Environment and Natural Resources, 639 pp. NC: Division of Marine Fisheries.
- Du, J., K. Park, T.M. Dallapenna, and J.M. Clay. 2019. Dramatic hydrodynamic and sedimentary responses in Galveston Bay and adjacent inner shelf to Hurricane Harvey. *Science of the Total Environment* 653: 554–564. <https://doi.org/10.1016/j.scitotenv.2018.10.403>.
- Edelsbrunner, H., D.G. Kirkpatrick, and R. Seidel. 1983. On the shape of a set of points in the plane. *IEEE Transactions on Information Theory* 29 (4): 551–559. <https://doi.org/10.1109/sfcs.1977.21>.
- Eulie, D.O., J.P. Walsh, D.R. Corbett, and R.P. Mulligan. 2017. Temporal and spatial dynamics of estuarine shoreline change in the Albemarle-Pamlico Estuarine System, North Carolina, USA. *Estuaries and Coasts* 40 (3): 741–757. <https://doi.org/10.1007/s12237-016-0143-8>.
- Eulie, D.O., D.R. Corbett, and J.P. Walsh. 2018. Shoreline erosion and decadal sediment accumulation in the Tar-Pamlico estuary, North Carolina, USA: a source-to-sink analysis. *Estuarine, Coastal and Shelf Science* 202: 246–258. <https://doi.org/10.1016/j.ecss.2017.10.011>.
- Feldens, P., I. Schulze, S. Papenmeier, M. Schönke, and J.S. von Deimling. 2018. Improved interpretation of marine sedimentary environments using multi-frequency multibeam backscatter data. *Geosciences* 8 (6): 214. <https://doi.org/10.3390/geosciences8060214>.
- Garg, L., P. Shukla, S.K. Singh, V. Bajpai, and U. Yadav. 2019. Land use land cover classification from satellite imagery using mUnet: a modified UNET architecture. *VISIGRAPP 2019 - Proceedings of the 14th International Joint Conference on Computer Vision, Imaging and Computer Graphics Theory and Applications* 4: 359–365. <https://doi.org/10.5220/0007370603590365>.
- Giffin, D., and D.R. Corbett. 2003. Evaluation of sediment dynamics in coastal systems via short-lived radioisotopes. *Journal of Marine*

- Systems* 42: 83–96. [https://doi.org/10.1016/S0924-7963\(03\)00068-X](https://doi.org/10.1016/S0924-7963(03)00068-X).
- Gonzalez, R.C., R.E. Woods, and S.L. Eddins. 2011. *Digital image processing using MATLAB*. New Jersey: Prentice Hall.
- Grabowski, J.H., R.D. Brumbaugh, R.F. Conrad, A.G. Keeler, J.J. Opaluch, C.H. Peterson, M.F. Piehler, S.P. Powers, and A.R. Smyth. 2012. Economic valuation of ecosystem services provided by oyster reefs. *BioScience* 62 (10): 900–909. <https://doi.org/10.1525/bio.2012.62.10.10>.
- Grizzle, R.E., and K.W. Ward. 2016. *Assessment of recent Eastern Oyster (Crassostrea virginica) reef restoration projects in the Great Bay Estuary, New Hampshire: planning for the future*. Final Report to Piscataqua Region Estuarine Partnership.
- Guan, S., A.A. Khan, S. Sikdar, and P.V. Chitnis. 2020. Fully dense UNet for 2-D sparse photoacoustic tomography artifact removal. *IEEE Journal of Biomedical and Health Informatics* 24 (2): 568–576. <https://doi.org/10.1109/JBHI.2019.2912935>.
- Haralick, R.M. 1974. A measure for circularity of digital figures. *IEEE Transactions on Systems, Man and Cybernetics* 4 (4): 394–396. <https://doi.org/10.1109/TSMC.1974.5408463>.
- Haralick, R.M., I. Dinstein, and K. Shanmugam. 1973. Textural features for image classification. *IEEE Transactions on Systems, Man and Cybernetics* 3 (6): 610–621. <https://doi.org/10.1109/TSMC.1973.4309314>.
- Hernández, A.B., R.D. Brumbaugh, P. Frederick, R. Grizzle, M.W. Luckenbach, C.H. Peterson, and C. Angelini. 2018. Restoring the eastern oyster: how much progress has been made in 53 years? *Frontiers in Ecology and the Environment* 16 (8): 463–471. <https://doi.org/10.1002/fee.1935>.
- Huff, L.C. 2008. Acoustic remote sensing as a tool for habitat mapping in Alaska waters. In *Marine habitat mapping technology for Alaska*, ed. J.R. Reynolds and H.G. Greene, 29–46. Fairbanks, AK, USA: Alaska Sea Grant, University of Alaska Fairbanks.
- Ji, Z.G., and K.R. Jin. 2014. Impacts of wind waves on sediment transport in a large, shallow lake. *Lakes and Reservoirs: Research and Management* 19 (2): 118–129. <https://doi.org/10.1111/lre.12057>.
- Jia, P., and M. Li. 2012a. Circulation dynamics and salt balance in a lagoonal estuary. *Journal of Geophysical Research: Oceans* 117 (C1): C01003. <https://doi.org/10.1029/2011JC007124>.
- Jia, P., and M. Li. 2012b. Dynamics of wind-driven circulation in a shallow lagoon with strong horizontal density gradient. *Journal of Geophysical Research: Oceans* 117 (C5): C05013. <https://doi.org/10.1029/2011JC007475>.
- La Peyre, M.K., A.T. Humphries, S.M. Casas, and J.F. La Peyre. 2014. Temporal variation in development of ecosystem services from oyster reef restoration. *Ecological Engineering* 63: 34–44. <https://doi.org/10.1016/j.ecoleng.2013.12.001>.
- Lenihan, H.S. 1999. Physical-biological coupling on oyster reefs: how habitat structure influences individual performance. *Ecological Monographs* 69: 251–275. [https://doi.org/10.1890/0012-9615\(1999\)069\[0251:PBCOOR\]2.0.CO;2](https://doi.org/10.1890/0012-9615(1999)069[0251:PBCOOR]2.0.CO;2).
- Lenihan, H.S., and C.H. Peterson. 1998. How habitat degradation through fishery disturbance enhances impacts of hypoxia on oyster reefs. *Ecological Applications* 8: 128–140. [https://doi.org/10.1890/1051-0761\(1998\)008\[0128:HHDTFD\]2.0.CO;2](https://doi.org/10.1890/1051-0761(1998)008[0128:HHDTFD]2.0.CO;2).
- Leonard, L.A., A.C. Hine, M.E. Luther, R.P. Stumpf, and E.E. Wright. 1995. Sediment transport processes in a west-central Florida open marine marsh tidal creek; the role of tides and extra-tropical storms. *Estuarine, Coastal and Shelf Science* 41 (2): 225–248. <https://doi.org/10.1006/ecss.1995.0063>.
- Li, R., W. Liu, L. Yang, S. Sun, W. Hu, F. Zhang, and W. Li. 2018. DeepUNet: a deep fully convolutional network for pixel-level sea-land segmentation. *IEEE Journal of Selected Topics in Applied Earth Observations and Remote Sensing* 11 (11): 3954–3962. <https://doi.org/10.1109/JSTARS.2018.2833382>.
- Lipcius, R.N., R.P. Burke, D.N. McCulloch, S.J. Schreiber, D.M. Schulte, R.D. Seitz, and J. Shen. 2015. Overcoming restoration paradigms: value of the historical record and metapopulation dynamics in native oyster restoration. *Frontiers in Marine Science* 2: 65. <https://doi.org/10.3389/fmars.2015.00065>.
- Liu, X., and W. Huang. 2009. Modeling sediment resuspension and transport induced by storm wind in Apalachicola Bay, USA. *Environmental Modelling and Software* 24 (11): 1302–1313. <https://doi.org/10.1016/j.envsoft.2009.04.006>.
- Lueck, R., L.St. Laurent, and J. Moun. 2019. Turbulence in the benthic boundary layer. In *Encyclopedia of ocean sciences*, ed. J.K. Cochran, H. Bokuniewicz, and P. Yager, 3rd ed. Elsevier Science & Technology.
- Luettich, R.A., S.D. Carr, J.V. Reynolds-Fleming, C.W. Fulcher, and J.E. McNinch. 2002. Semi-diurnal seiche in a shallow, micro-tidal lagoonal estuary. *Continental Shelf Research* 22 (11-13): 1669–1681. [https://doi.org/10.1016/S0278-4343\(02\)00031-6](https://doi.org/10.1016/S0278-4343(02)00031-6).
- MD DNR. 2020. Ecological restoration. Maryland Department of Natural Resources. <https://dnr.maryland.gov/fisheries/Pages/oysters/ecorrestoration.aspx>. Accessed 3 February 2020.
- Mroch, R.M., D.B. Eggleston, and B.J. Puckett. 2012. Spatiotemporal variation in oyster fecundity and reproductive output in a network of no-take reserves. *Journal of Shellfish Research* 31 (4): 1091–1101. <https://doi.org/10.2983/035.031.0420>.
- Mulligan, R.P., J.P. Walsh, and H.M. Wadman. 2015. Storm surge and surface waves in a shallow lagoonal estuary during the crossing of a hurricane. *Journal of Waterway, Port, Coastal, and Ocean Engineering* 141 (4): A5014001. [https://doi.org/10.1061/\(ASCE\)WW.1943-5460.0000260](https://doi.org/10.1061/(ASCE)WW.1943-5460.0000260).
- NC DMF. 2020a. Habitat enhancement programs. North Carolina Environmental Quality Division of Marine Fisheries. <http://portal.ncdenr.org/web/mf/habitat/enhancement>. Accessed 31 January 2020.
- NC DMF. 2020b. Estuarine benthic mapping program. North Carolina Environmental Quality Division of Marine Fisheries. <http://portal.ncdenr.org/web/mf/habitat/maps>. Accessed 25 September 2020.
- NC DWR. 2009. Neuse River basinwide water quality plan. North Carolina Division of Water Resources. <https://www.ncwater.org/basins/neuse/index01072015.php>. Accessed 7 February 2020.
- NC DWR. 2014. Tar-Pamlico River basinwide water resources management plan. North Carolina Division of Water Resources. <https://www.ncwater.org/basins/Tar-Pamlico/index.php>. Accessed 7 February 2020.
- Olofsson, P., G.M. Foody, S.V. Stehman, and C.E. Woodcock. 2013. Making better use of accuracy data in land change studies: estimating accuracy and area and quantifying uncertainty using stratified estimation. *Remote Sensing of Environment* 129: 122–131. <https://doi.org/10.1016/j.rse.2012.10.031>.
- Olofsson, P., G.M. Foody, M. Herold, S.V. Stehman, C.E. Woodcock, and M.A. Wulder. 2014. Good practices for estimating area and assessing accuracy of land change. *Remote Sensing of Environment* 148: 42–57. <https://doi.org/10.1016/j.rse.2014.02.015>.
- Olofsson, P., P. Arévalo, A.B. Espejo, C. Green, E. Lindquist, R.E. McRoberts, and M.J. Sanz. 2020. Mitigating the effects of omission errors on area and area change estimates. *Remote Sensing of Environment* 236: 111492. <https://doi.org/10.1016/j.rse.2019.111492>.
- Osburn, C.L., J.C. Rudolph, H.W. Paerl, A.G. Hounshell, and B.R. Van Dam. 2019. Lingering carbon cycle effects of Hurricane Matthew in North Carolina's coastal waters. *Geophysical Research Letters* 46 (5): 2654–2661. <https://doi.org/10.1029/2019GL082014>.
- Pace, N.G., and C.M. Dyer. 1979. Machine classification of sedimentary sea bottoms. *IEEE Transactions on Geoscience Electronics* 17 (3): 52–56. <https://doi.org/10.1109/TGE.1979.294612>.
- Paerl, H.W., J.L. Pinckney, J.M. Fear, and B.L. Peierls. 1998. Ecosystem responses to internal and watershed organic matter loading: consequences for hypoxia in the eutrophying Neuse River Estuary, North Carolina, USA. *Marine Ecology Progress Series* 166: 17–25. <https://doi.org/10.3354/meps166017>.

- Paerl, H.W., L.M. Valdes, A.R. Joyner, B.L. Peierls, M.F. Piehler, S.R. Riggs, R.R. Christian, L.A. Eby, L.B. Crowder, J.S. Ramus, E.J. Clesceri, C.P. Buzzelli, and R.A. Luettich. 2006. Ecological response to hurricane events in the Pamlico Sound system, North Carolina, and implications for assessment and management in a regime of increased frequency. *Estuaries and Coasts* 29 (6): 1033–1045. <https://doi.org/10.1007/bf02798666>.
- Paerl, H.W., J.R. Crosswell, B. Van Dam, N.S. Hall, K.L. Rossignol, C.L. Osburn, A.G. Hounshell, R.S. Sloup, and L.W. Harding. 2018. Two decades of tropical cyclone impacts on North Carolina's estuarine carbon, nutrient and phytoplankton dynamics: implications for biogeochemical cycling and water quality in a stormier world. *Biogeochemistry* 141 (3): 307–332. <https://doi.org/10.1007/s10533-018-0438-x>.
- Paerl, H.W., N.S. Hall, A.G. Hounshell, K.L. Rossignol, M.A. Barnard, R.A. Leuttich, J.C. Rudolph, C.L. Osburn, J. Bales, and L.W. Harding. 2020. Recent increases of rainfall and flooding from tropical cyclones (TCs) in North Carolina (USA): implications for organic matter and nutrient cycling in coastal watersheds. *Biogeochemistry* 150 (2): 197–216. <https://doi.org/10.1007/s10533-020-00693-4>.
- Peters, J.W., D.B. Eggleston, B.J. Puckett, and S.J. Theuerkauf. 2017. Oyster demographics in harvested reefs vs. no-take reserves: implications for larval spillover and restoration success. *Frontiers in Marine Science* 4: 326. <https://doi.org/10.3389/fmars.2017.00326>.
- Pierson, K.J., and D.B. Eggleston. 2014. Response of estuarine fish to large-scale oyster reef restoration. *Transactions of the American Fisheries Society* 143 (1): 273–288. <https://doi.org/10.1080/00028487.2013.847863>.
- Pollack, J.B., A. Cleveland, T.A. Palmer, A.S. Reisinger, and P.A. Montagna. 2012. A restoration suitability index model for the Eastern Oyster (*Crassostrea virginica*) in the Mission-Aransas Estuary, TX, USA. *PLoS ONE* 7 (7): e40839. <https://doi.org/10.1371/journal.pone.0040839>.
- Poppe, L.J., K.Y. McMullen, S.J. Williams, and V.F. Paskevich. 2014. USGS east-coast sediment analysis: procedures, database, and GIS data (ver. 3.0, November 2014): U.S. *Geological Survey open-file report 2005-1001* <https://pubs.usgs.gov/of/2005/1001/>.
- Powers, S.P., C.H. Peterson, J.H. Grabowski, and H.S. Lenihan. 2009. Success of constructed oyster reefs in no-harvest sanctuaries: implications for restoration. *Marine Ecology Progress Series* 389: 159–170. <https://doi.org/10.3354/meps08164>.
- Puckett, B.J., and D.B. Eggleston. 2012. Oyster demographics in a network of no-take reserves: recruitment, growth, survival, and density dependence. *Marine and Coastal Fisheries* 4 (1): 605–627. <https://doi.org/10.1080/19425120.2012.713892>.
- Puckett, B.J., and D.B. Eggleston. 2016. Metapopulation dynamics guide marine reserve design: importance of connectivity, demographics, and stock enhancement. *Ecosphere* 7 (6): e01322. <https://doi.org/10.1002/ecs2.1322>.
- Puckett, B.J., D.B. Eggleston, P.C. Kerr, and R.A. Luettich. 2014. Larval dispersal and population connectivity among a network of marine reserves. *Fisheries Oceanography* 23 (4): 342–361. <https://doi.org/10.1111/fog.12067>.
- Puckett, B.J., S.J. Theuerkauf, D.B. Eggleston, R. Guajardo, C. Hardy, J. Gao, and R.A. Luettich. 2018. Integrating larval dispersal, permitting, and logistical factors within a validated Habitat Suitability Index for oyster restoration. *Frontiers in Marine Science* 5: 76. <https://doi.org/10.3389/FMARS.2018.00076>.
- Quo, Z., L. Zhang, L. Lu, M. Bagheri, R.M. Summers, M. Sonka, and J. Yao. 2018. Deep LOGISMOS: Deep learning graph-based 3D segmentation of pancreatic tumors on CT scans. *Proceedings - International Symposium on Biomedical Imaging*, 2018-April: 1230–1233. <https://doi.org/10.1109/ISBI.2018.8363793>.
- Reed, T.B., and D. Hussong. 1989. Digital image processing techniques for enhancement and classification of Sea MARC II side scan sonar imagery. *Journal of Geophysical Research* 94 (B6): 7469–7490. <https://doi.org/10.1029/JB094iB06p07469>.
- Reidenbach, M.A., M. Limm, M. Hondzo, and M.T. Stacey. 2010. Effects of bed roughness on boundary layer mixing and mass flux across the sediment-water interface. *Water Resources Research* 46 (7): W07530. <https://doi.org/10.1029/2009WR008248>.
- Ronneberger, O., P. Fischer, and T. Brox. 2015. U-net: Convolutional networks for biomedical image segmentation. *Lecture Notes in Computer Science (including subseries Lecture Notes in Artificial Intelligence and Lecture Notes in Bioinformatics)* 9351: 234–241. https://doi.org/10.1007/978-3-319-24574-4_28.
- Schulte, D.M., R.P. Burke, and R.N. Lipcius. 2009. Unprecedented restoration of a native oyster metapopulation. *Science* 325 (5944): 1124–1128. <https://doi.org/10.1126/science.1176516>.
- Stehman, S.V. 2013. Estimating area from an accuracy assessment error matrix. *Remote Sensing of Environment* 132: 202–211. <https://doi.org/10.1016/j.rse.2013.01.016>.
- Stoian, A., V. Poulain, J. Inglada, V. Poughon, and D. Derksen. 2019. 1986. Land cover maps production with high resolution satellite image time series and convolutional neural networks: adaptations and limits for operational systems. *Remote Sensing* 11. <https://doi.org/10.3390/rs11171986>.
- Stokes, S., S. Wunderink, M. Loew, G. Gereffi. 2012. Restoring gulf oyster reefs: opportunities and innovation, Duke University, Global Value Chains, Available online: <https://gvcc.duke.edu/cggclisting/restoring-gulf-oyster-reefs-opportunities-for-innovation/>
- Styles, R. 2015. Flow and turbulence over an oyster reef. *Journal of Coastal Research* 314: 978–985. <https://doi.org/10.2121/jcoastres-d-14-00115.1>.
- Theuerkauf, S.J., and R.N. Lipcius. 2016. Quantitative validation of a habitat suitability index for oyster restoration. *Frontiers in Marine Science* 3: 64. <https://doi.org/10.3389/fmars.2016.00064>.
- Theuerkauf, S.J., D.B. Eggleston, and B.J. Puckett. 2019. Integrating ecosystem services considerations within a GIS-based habitat suitability index for oyster restoration. *PLOS ONE* 14 (1): e0210936. <https://doi.org/10.1371/journal.pone.0210936>.
- VA DEQ. 2020. Coastal issues & Virginia Coastal Zone Management program initiatives. Virginia Department of Environmental Quality. <https://www.deq.virginia.gov/Programs/CoastalZoneManagement/CZMIssuesInitiatives.aspx>. Accessed 3 February 2020.
- Wells, J.T., and S.Y. Kim. 1989. Sedimentation in the Albemarle-Pamlico lagoonal system: synthesis and hypotheses. *Marine Geology* 88 (3-4): 263–284. [https://doi.org/10.1016/0025-3227\(89\)90101-1](https://doi.org/10.1016/0025-3227(89)90101-1).
- Whitman, E.R., and M.A. Reidenbach. 2012. Benthic flow environments affect recruitment of *Crassostrea virginica* larvae to an intertidal oyster reef. *Marine Ecology Progress Series* 463: 177–191. <https://doi.org/10.3354/meps09882>.
- Xie, L., and D.B. Eggleston. 1999. Computer simulations of wind-induced estuarine circulation patterns and estuary-shelf exchange processes: the potential role of wind forcing on larval transport. *Estuarine, Coastal and Shelf Science* 49 (2): 221–234. <https://doi.org/10.1006/ecss.1999.0498>.
- Xue, Z., R. He, J.P. Liu, and J.C. Warner. 2012. Modeling transport and deposition of the Mekong River sediment. *Continental Shelf Research* 37. Pergamon: 66–78. <https://doi.org/10.1016/j.csr.2012.02.010>.
- Zang, Z., Z.G. Xue, N. Bi, Z. Yao, X. Wu, Q. Ge, and H. Wang. 2017. Seasonal and intra-seasonal variations of suspended-sediment distribution in the Yellow Sea. *Continental Shelf Research* 148: 116–129. <https://doi.org/10.1016/j.csr.2017.08.016>.
- Zyuzin, V., P. Sergey, A. Mukhtarov, T. Chumamaya, O. Solovyova, A. Bobkova, and V. Myasnikov. 2018. Identification of the left ventricle endocardial border on two-dimensional ultrasound images using the convolutional neural network Unet. *Proceedings - 2018 Ural Symposium on Biomedical Engineering, Radioelectronics and Information Technology, USBEREIT 2018*: 76–78. <https://doi.org/10.1109/USBREIT.2018.8384554>.